Hovenga Paige (Orcid ID: 0000-0002-3569-0123)

The relative role of constructive and destructive processes in dune evolution on Cape Lookout National Seashore, North Carolina, USA

Running title: Constructive-destructive processes of dune evolution

Paige A. Hovenga,[1]* Peter Ruggiero,[2] Evan B. Goldstein,[3] Sally D. Hacker,[4] and Laura J. Moore[5]

[1] School of Civil and Construction Engineering, Oregon State University, Corvallis, Oregon, USA

[2] College of Earth, Ocean, and Atmospheric Sciences, Oregon State University, Corvallis, Oregon, USA

[3] Department of Geography, Environment, and Sustainability, University of North Carolina at Greensboro, Greensboro, North Carolina, USA

[4] Department of Integrative Biology, Oregon State University, Corvallis, Oregon, USA

[5] Department of Geological Sciences, University of North Carolina at Chapel Hill, Chapel Hill, North Carolina, USA

*Corresponding Author: Paige Hovenga, email address: hovengap@oregonstate.edu, phone: (954) 404-2588, 101 SW 26th St., Corvallis, Oregon, USA 97331

Acknowledgments: This work was funded by NOAA via the NOS/NCCOS/CRP Ecological Effects of Sea-Level Rise Program (grant no. NA15NOS4780172) to P.R.,

S.D.H., and L.J.M. and by the U.S. Coastal Research Program (USCRP) Cooperative Agreement Number W12HZ2020009 to P.R. and P.H.

Author Contributions: Conceptualization: P.R., S.D.H., L.J.M., E.B.G.; funding acquisition: P.R., S.D.H., L.J.M., P.H.; methodology: P.R. P.H., E.B.G; investigation: P.H. and P.R., resources: P.R. software: P.H. and P.R.; supervision: P.R., S.D.H., L.J.M.; writing – original draft preparation: P.H. and P.R.; writing – review and editing: P.H., P.R., E.B.G., S.D.H., L.J.M. All authors have read and agreed to the submitted version of the manuscript.

Data Availability Statement: Lidar data are available through the National Oceanic and Atmospheric Administration (NOAA) Digital Coast website (NOAA Digital Coast, 2016). Wave, wind, and water level data are provided by the U.S. Army Corps of Engineers Wave Information Study (U.S. Army Corps. of Engineers, 1997), the NOAA National Data Buoy Center (Cape Lookout, NC Station: CLKN7; NOAA's National Data Buoy Center, 2020), and the NOAA Tide and Currents website (Beaufort, Duke Marine Lab Station ID: 8656483; NOAA Tide & Currents, 2020).

The relative role of constructive and destructive processes in dune evolution on Cape Lookout National Seashore, North Carolina, USA

Abstract

Coastal dunes are dynamic features that are continuously evolving due to constructive (e.g., wind and wave driven sediment transport) and destructive (e.g., elevated total water levels during storm events) processes. However, the relative importance of these processes in determining dune evolution is often poorly understood. In this study, ten lidar datasets from 1997-2016 are used to determine the relative role of erosion and accretion processes driving foredune change on the coast of Cape Lookout National Seashore, North Carolina, USA. Beach and dune morphometrics reveal that dune toe locations have generally retreated since 1997 while dune crest heights accreted by 0.01-0.02 m/yr. We develop three univariate metrics that represent (1) the potential for erosion, i.e., total water level impact hours per year, (2) accretion, i.e., dune building hours per year, and (3) the relative net effect of foredune accretion and erosion processes, i.e., constructive-destructive dune forcing (CDDF) ratio, and test the correlative power of these metrics in explaining changes in foredune morphology. The total water level impact hours per year metric explained as much as 66% and 67% of the variance in dune crest and toe elevations, respectively, across the nearly two decades of dune evolution. The greatest number of dune building hours per

year and largest dunes within the study site co-occurred at locations exposed to the dominant cross-shore wind direction as a result of varying shoreline orientation. The CDDF ratio was positively correlated to changes in the dune toe elevation in approximately 70% of dunes within the study site, outperforming the impact and dune building hours per year metrics. Our results show that these three metrics can provide first order estimates of dune morphometric change across multiple spatial and temporal scales, which may be particularly useful at sites where lidar acquisition is intermittent.

Keywords: foredune evolution; dune morphology; total water level; dune building; alongshore variability

1 Introduction

Coastal dunes provide an important set of ecosystem services including defense from surge and waves during storm events, habitat for wildlife, tourism, recreation, and carbon sequestration (Barbier et al., 2011; Spurgeon, 1999). Natural dunes are highly dynamic features which are constantly changing in response to erosion from storm events and subsequently recovering during calmer periods via aeolian and wave driven sediment transport (Cohn et al., 2019a, 2019b; Durán Vinent and Moore, 2015; Goldstein and Moore, 2016; Halls et al., 2018; Hosier and Cleary, 1977; Houser and Hamilton, 2009; Mitasova et al., 2009; Ritchie and Penland, 1988; Sallenger et al., 2006). Predicting the intensity, rate, and frequency of these changes is complicated by factors such as the antecedent geology, pre-existing dune morphology, mean sea level,

tidal range, wind and wave climate, sediment supply, sand moisture level, other sediment supply limiters, and dune ecological characteristics (Arens et al., 2001; Charbonneau et al., 2017; Davidson-Arnott and Law, 1990; de Vries et al., 2014; Durán and Moore, 2013; Hacker et al., 2019; Hesp, 1989; Houser and Hamilton, 2009; Psuty, 1988; Riggs et al., 2011; Sallenger, 2000; Seabloom et al., 2013; Short and Hesp, 1982).

Conceptual models, often coupled with empirical data, have been used to describe the general behavior of dune development as it relates to sediment availability, storm hydrodynamics, and vegetation characteristics (Biel et al., 2019; Davidson-Arnott and Law, 1990; Hacker et al., 2012; Psuty, 1988; Ruggiero et al., 2018; Sallenger, 2000; Short and Hesp, 1982; Zarnetske et al., 2012). For example, the early model of Short and Hesp (1982) relates potential foredune size with different beach types (i.e., reflective to dissipative) and wave and wind driven sediment transport. Wide dissipative beaches, as opposed to reflective beaches, are argued to have the largest dunes due to the high potential for wave driven sediment transport associated with low mobility, wide fetches, and low beach slopes. While existing conceptual and empirically based models provide fundamental insights into beach-dune systems, they are generally limited to a qualitative understanding of beach and dune evolution, often considering only constructive (dune-building) or destructive (dune-eroding) processes driving foredune

change, and are typically unable to resolve high resolution spatial variability (Cohn et al., 2019a; Houser, 2009; Roelvink and Costas, 2019; Sherman and Bauer, 1993).

Emerging numerical dune evolution models including the Coastal Dune Model (CDM) (Durán and Moore, 2013), DUne BEach VEGetation (DUBEVEG) (Keijsers et al., 2016), the model developed by Davidson-Arnott et al. (2018), and Duna (Roelvink and Costas, 2019) yield quantitative assessments of the erosive and accretional responses of beaches and dunes and incorporate processes related to vegetative effects, sand moisture, grain size variability, and bed slope interactions. Recent efforts have coupled dune evolution models with nearshore hydro-morphodynamic models (e.g., Windsurf; Cohn et al., 2019a, XBeach-Duna; Roelvink and Costas, 2019, and the cross-shore (CS) model; Larson et al., 2016) to coevolve the beach-dune system in a more holistic manner. These state-of-the-art models may provide transformative tools for better predicting future coastal hazards and guiding resiliency planning as they can also be adapted to incorporate management decisions such as beach nourishment, dune construction, and dune grass planting designs (Ruggiero et al., 2019). However, this burgeoning suite of models often requires *in-situ* datasets or knowledge of local boundary conditions that can be difficult and costly to acquire. Additionally, these tools are still in their infancy, and their prediction horizons and applicability at varying spatial resolutions are still being assessed. Therefore, to improve the robustness of foredune morphologic change estimates at varying temporal (interannual to decadal) and spatial

(meters to tens of kilometers) scales, there is still a need to better understand the relative contributions of constructive and destructive processes driving variable dune evolution.

Remote sensing techniques, including airborne lidar, can provide fundamental datasets for which the coupled processes that drive natural dune evolution, and the varying frequencies and spatial scales at which they occur, can be evaluated. Automated techniques to extract dune morphometrics from lidar provide a way to characterize large areas of the coast at high spatial resolutions, which can be used for flood zone delineation, monitoring beach-nourishment projects, and mapping barrier island changes (Beuzen, 2019; Elko et al., 2002; Klemas, 2011; Mull and Ruggiero, 2014; Stockdon et al., 2009). Additionally, increasingly available wind, wave, and water level data from offshore buoys, meteorological stations, and model hindcasts/forecasts, coupled with snapshots of beach and dune morphology extracted from lidar, can be used to develop techniques that provide first-order estimates of morphological change.

In this study, we use ten airborne lidar datasets collected over nearly 20 years (1997-2016) to determine the relative role of constructive and destructive processes driving foredune evolution on a vulnerable shoreline at Cape Lookout National Seashore, North Carolina, USA. Specifically, we ask:

1) How have beaches and foredunes at Cape Lookout National Seashore, North Carolina, USA changed at varying temporal (interannual to decadal) and spatial (meters to tens of kilometers) scales?

2) Can we collapse complex coupled processes that drive foredune evolution into univariate metrics related to erosion and accretion of dunes to better understand the alongshore variability and temporal change of coastal foredunes?

To address these questions we develop three univariate metrics, derived from complex multivariate drivers that represent the general destructive and constructive processes significant for beach and foredune evolution. The metrics include: (1) total water level impact hours per year, a measure of the potential for erosion of the foredune, (2) dune building hours per year, a measure of the potential for sand accretion on the foredune, and (3) the constructive-destructive dune forcing (CDDF) ratio, a measure representing the relative importance of processes driving foredune accretion and erosion. The correlation between the impact and dune building metrics, both individually and collectively, and the changes in foredune morphology are evaluated for spatially and temporally varying morphologic and environmental conditions.

2 Study Site

The study region consists of three low-lying barrier islands: Shackleford Banks (SHB), South Core Banks (SCB), and North Core Banks (NCB) (Figure 1). The 90

kilometer stretch of coast comprises the Cape Lookout National Seashore (CALO). The barrier islands are separated by a series of inlets including Barden Inlet (between Shackleford and South Core Banks), initially breached during the 1933 Outer Banks Hurricane and subsequently dredged by the U.S. Army Corps of Engineers (USACE), and Ophelia Inlet (between North and South Core Banks), which opened in 2005 due to Hurricane Ophelia (Park and Wells, 2005; Wells, 1988). New Drum Inlet located approximately one kilometer (km) north of Ophelia Inlet, was originally opened in 1971 by the USACE and New-Old Drum Inlet, around five kms north of Ophelia Inlet and formerly referred to as Drum Inlet, was breached in 1999 by Hurricane Dennis (Mallinson et al., 2008). New Drum Inlet and New-Old Drum Inlet have been repeatedly opened, closed, and reworked by waves.

Mean sea level measured at Beaufort, Duke Marine Lab (National Oceanic and Atmospheric Administration's (NOAA) Station: 8656483) has been rising at a rate of 3.10 ± 0.35 millimeters/year from 1953-2018 (Figure 2). The micro-tidal range is approximately 0.95 meters (m) and is mixed, dominantly semi-diurnal. Historical wave hindcasts made by the USACE Wave Information Study (WIS) show the seasonal dominant wave direction is from the east during the fall and winter and from the south in the spring and summer (Park and Wells, 2005; U.S. Army Corps. of Engineers, 1997). The average seasonal wave height and period is 1.4 m and 5.8 seconds (s) during the winter and 1.1 m and 5.3 s in the summer (Park and Wells, 2005). WIS hindcasts show

that wave height and direction vary in magnitude and direction in the alongshore (Figure 2).

Park and Wells (2005) describe a well-defined seasonal wind pattern with north to northeast winds in the winter and fall and southwest and northeast winds in the spring and summer. The alongshore variability in the WIS hindcast wind speed and direction is less than that of the wave climate (Figure 2). The NOAA weather station (CLKN7), located on the southern tip of South Core Banks, measured slightly weaker winds from 1997-2017 compared to the WIS hindcasts but exhibited the same dominant wind direction (Figure 2). This region is frequently impacted by destructive surges and waves during storm events including nor'easters, which typically occur between the months of December to March, and from hurricanes, which occur during the summer and fall months (Dolan and Lins, 1985).

CALO was established as a National Seashore in 1966 and has remained relatively undeveloped and without significant management actions (e.g., nourishment, armoring, grass planting) altering the beaches and dunes. Therefore, CALO is an ideal region for studying natural dune evolution and the driving forces behind it due to the preservation of the natural beach-dune system, repeated cycles of response to storms and recovery periods, and spatial variability in the geomorphology, shoreline orientation, and environmental forcing conditions (Godfrey, 1976; Hovenga et al., 2019).

3 Methodology

3.1 Beach and Foredune Morphometric Extraction

Beach and dune morphometrics (i.e., shoreline position, beach slope, beach width, dune toe, crest, and heel height and location, and dune volume) were extracted from ten airborne lidar datasets between 1997-2016 using methods modified from Mull and Ruggiero (2014) (Figure 3). The lidar datasets were acquired from NOAA's Digital Coast website (2016), and details for each dataset are provided in Table S1. Cross-shore profiles were cast at 40 m along-shore intervals across the study site, totaling 2,298 transects (i.e., 369 along SHB, 1,053 along SCB, and 876 along NCB) for each of the ten lidar datasets. Details about the lidar datasets, exaction methods, and associated horizontal and vertical errors are provided in the Supporting Information.

3.2 Foredune Erosion Metric – Total Water Level Impact Hours Per Year

To assess the impact of destructive environmental forces on beach and dune morphology, we calculated the total water level (TWL) impact hours per year (e.g., Ruggiero et al., 2001; Wahl et al., 2016; Wahl and Plant, 2015), a measure of foredune erosion potential. To do so, spatially varying, hourly TWLs were estimated from 01/01/1998-12/31/2017 by combining observed still water levels (SWLs) with empirical estimates of wave runup (Ruggiero et al., 2001). This time period was selected to provide TWLs for full, complete years following when the first and last lidar datasets

were collected; note the acquisition of the first lidar dataset was completed in October 1997. Observed SWLs were obtained from the NOAA tide gauge at Beaufort, NC (8656483) and hindcast wave heights, periods, and directions were acquired from ten USACE WIS nodes at approximately 20-30 m depths (Figure 2). WIS stations were assigned to each transect based on the closest proximity to a shore-normal extension of the profile offshore. To address sheltering effects due to the varying shoreline orientation within the study site, waves approaching beyond ± 90º to the shore-normal angle were excluded. The two percent exceedance elevation of wave runup ($R_{2\%}$) was calculated with the Stockdon et al. (2006) formulation using the wave heights and periods from the assigned WIS station and the most up to date foreshore beach slopes extracted from the lidar datasets. A representative example of the TWL and its constituents at three different locations within the study site are shown in Figure S1.

The TWL time series and lidar extracted dune toe and crest elevations at each transect were used to estimate the hourly storm impact regimes (i.e., collision and overwash as uniquely independent regimes) from 1998-2017 at each transect using the storm impact scaling model from Sallenger (2000). The dune toe and crest elevations and foreshore slopes were updated in the time series at the date of completion of each lidar survey (Table S1) and were held constant between lidar surveys. We aggregated the number of hours per year (hpy) each transect was predicted to be in the collision regime and in the overwash regime to estimate the TWL impact hours per year. The

implications of using a stationary SWL, constant dune morphology as opposed to time evolving between lidar datasets, and the beach state during the collection of each lidar dataset (i.e., post-storm conditions versus recovered) are reviewed in the Discussion section.

We compiled a list of the 23 extreme or named extratropical storms, tropical depressions, tropical storms, and hurricanes passing within a 100 km radius of Cape Lookout National Seashore between 1997 and 2017 (Table 1) (NOAA Digital Coast, 2018). To explore how impactful each storm was, we identified the maximum TWL and SWL that occurred within the study area during each event. Additionally, the TWL time series at each transect was used to calculate the five, independent, largest TWL events per year (i.e., totaling 100 TWL events from 1997-2017 at each transect). We compared the date of occurrence for each named storm (Table 1) to those of the site-specific TWL events and calculated the percent of the total transects within the study region for which each named storm was associated with the five largest TWL events at each location.

3.3 Foredune Accretion Metric – Dune Building Hours Per Year

To assess dune accretion as a result of aeolian sediment transport, we developed a univariate metric that represents the number of potential dune building hours per year. To be considered a dune building hour, the following criteria, populated with values from the literature, had to be met: 1) the fetch length, F, calculated as the cross-shore

distance from the hourly time and space varying TWLs at each transect (section 3.2) to the lidar extracted dune toe location, had to be greater than or equal to half a critical fetch length, F_c (Bauer and Davidson-Arnott, 2003; de Vries et al., 2014; Delgado-Fernandez, 2010), 2) the wind velocity had to be equal to or exceed a threshold velocity for sediment entrainment (Bagnold, 1941), and 3) both conditions 1) and 2) had to be met for a specified number of consecutive hours (Delgado-Fernandez and Davidson-Arnott, 2011). Critical fetch lengths found in previous field studies range from 10's to 100's of meters and may vary with wind velocity and other supply limiting factors, e.g., surface moisture and sediment sorting (Bauer et al., 2009; Davidson-Arnott et al., 2018; Davidson-Arnott and Law, 1990; Delgado-Fernandez, 2010; Lynch et al., 2008; Nordstrom and Jackson, 1992; Svasek and Terwindt, 1974; Walker, 2020). For this study, we used a F_c of 20 m, which was within the range of values reported by Svasek and Terwindt (1974; F_c = 10-20 m) and Davidson-Arnott and Law (1990; F_c ranged from 10-15 m for winds slightly greater than the threshold velocity to greater than 40 m for winds exceeding 14 m/s). We imposed a minimum duration of 2 consecutive hours (Delgado-Fernandez and Davidson-Arnott, 2011). A threshold velocity of 6.0 m/s was calculated using methods outlined by Delgado-Fernandez and Davidson-Arnott (2011) (Equation S5) for an average sand surface grain size of 0.3 mm (Hovenga et al., 2019) and wind velocities measured at a 9.8 m elevation (NOAA CLKN7 weather station; Figure 2) (Bagnold, 1941; Belly, 1964; Delgado-Fernandez and Davidson-Arnott, 2011;

Fryberger and Dean, 1979; Lettau and Lettau, 1977). Wind speeds and directions from the NOAA CLKN7 weather station were used to calculate the magnitude of onshore directed wind speed using a localized shoreline orientation that was measured across a 400 m length scale in the alongshore. The velocity of winds approaching outside ± 90º to shore-normal were considered unable to build dunes. The observed data was 97% complete for the study time period thus data gaps were filled using wind speeds and directions from WIS station 63272 following a bias correction based on the monthly average wind speed at both the CLKN7 and WIS 63272 stations. The sensitivity of the number of dune building hours per year to the critical fetch length (i.e., 15-25 m), threshold velocity (i.e., 5-7 m/s), and minimum number of consecutive (i.e., 1-3 hours) is provided in the Supporting Information. While other limiting factors including sediment availability, armoring, surface moisture, and spatially varying velocity gradients (Cohn et al., 2019a; Hallin et al., 2019; Hoonhout and Vries, 2016; Moore et al., 2016) are likely to impact the utility of these metrics, exploration of these factors is beyond the scope of this study.

3.4 Net Effect of Foredune Accretion and Erosion Metric

The dune building hours and the TWL impact hours were combined to quantify the potential net effect of foredune accretion and erosion. The constructive-destructive dune forcing (CDDF) ratio, was calculated as:

$$CDDF_i\ (\%) = 100\left(\frac{Dune\ building\ hpy_i - TWL\ Impact\ hpy_i}{\#\ of\ hours\ in\ each\ year}\right) \quad (1)$$

CDDF represents the percent of each year *i*, from 1998-2017, that each transect experienced a constructive state (i.e., more dune building than TWL impact hours per year) versus a destructive state (i.e., more TWL impact than dune building hours per year). The sign of the ratio indicates whether foredunes had more accretion potential (positive) or more erosion potential (negative), and the absolute value represents the magnitude of the potential change.

3.5 Relative Importance of Constructive Versus Destructive Processes in Foredune Evolution

The correlation between the constructive and destructive metrics (i.e., number of impact hours per year, dune building hours per year, and the CDDF ratio) and foredune morphology (i.e., dune toe and crest elevations) were evaluated at a variety of locations and spatial extents (i.e., single transect, two-kilometers, and 20-kilometers). Additionally, we calculated the percent of the total transects between kms 4-14 on SHB (250 transects), kms 8-36 on SCB (700 transects), and kms 7-27 on NCB (500 transects) with a significant correlation at the 95% confidence level between the three forcing metrics and the dune morphometrics. These regions were chosen to exclude areas adjacent to inlets where low lying dunes and vast overwash plains exist.

4 Results

4.1 Beach and Foredune Morphometrics

The beach and dune morphology differed between Shackleford Banks (SHB), South Core Banks (SCB), and North Core Banks (NCB) (Figure 4). SHB hosts taller and steeper dunes with greater sand volumes than the other islands, and the beaches had narrower beach widths and steeper foreshore and backshore beach slopes. Overall, SHB had the most variable dune crest elevations while SCB and NCB had a bimodal distribution. Between 1997 and 2016 dune crests became less variable on SHB and more variable on SCB and NCB. Over the nearly two decades, dune crests grew an average of 0.39, 0.46, and 0.31 m on SHB, SCB, and NCB, respectively (Table S3). Note, these decadal scale magnitudes of change are statistically significant when compared to regionally averaged, decadal endpoint rate uncertainty (Table S2).

Dune toe elevations increased and partial dune volumes (volume measured between the dune toe and crest; Figure 3) decreased on SHB and SCB from 1997-2016 (Figure 4b and c). On SHB, backshore slopes increased by an average of 0.01 and beach widths decreased (Figure 4f and g). Contrastingly on NCB, dune toe elevations decreased and became less varied (Figure 4b and Table S3). Additionally, the beaches widened and partial dune volumes increased. On all three islands, vertical dune crest accretion (Figure 4a), combined with general retreat of the dune toe (Figure 5a), resulted in steeper dune faces, of which SHB had the steepest. Between 1997 to 2016,

total dune volumes (volume measured between the dune toe and heel; Figure 3) increased more on SCB and NCB than on SHB (Figure 4e).

4.2 Interannual to Decadal Rates of Foredune Change

We calculated the interannual (2011-2016) to decadal (1997-2016) change rate of foredune morphology represented by the dune toe cross-shore location (relative to the 1997 position) and dune crest elevation (Figure 5). The decadal response was calculated using an endpoint rate between the 1997 and 2016 lidar datasets, and the interannual rate was determined using a linear regression through the 2011, 2012, 2014, and 2016 lidar datasets. The regionally averaged change rates and the percent of individual transects with a significant change rate are provided in the Supporting Information. At the decadal timescale, all three islands experienced net retreat at the dune toe, with SHB experiencing the largest retreat rates (average equal to -2.2 ± 0.06 m/yr) compared to SCB (-1.7 ± 0.03 m/yr) and NCB (-0.9 ± 0.03 m/yr) (Figure 5a; Table S2). Dunes had the greatest rates of erosion, as much as -20 m/yr, on the west end of SHB between kms 0-4 in the alongshore. The rate of dune toe retreat on SCB was also high north of km 36 near Ophelia Inlet. The trends exhibited by the cross-shore position of dune toes were related to the observed changes in the cross-shore location of the shoreline relative to the 1997 position (not shown; coefficient of determination, R^2 = 0.57) and cross-shore position of the dune crest (not shown; R^2 = 0.94). The rates of change were more variable at the interannual scale than at the decadal scale (Figure

5a). Dune toe retreat was most rapid on SHB (-6.3 m/yr) at the interannual time scale; however, this rate was largely influenced by the significant erosion on the western end. East of km 4, the average dune toe retreat rate was -0.1 m/yr. As much as -30 m/yr of dune toe erosion occurred on the northern extents of SCB and NCB (Figure 5a). Large signals of dune toe progradation (as much as 30 m/yr) were also observed. NCB had a net progradation of 2.0 m/yr, with amplified rates of 4.8 m/yr between kms 17-30.

Dune crests on SHB, SCB, and NCB accreted on the decadal timescale at rates of 0.02, 0.02, and 0.01 m/yr (± 0.001 m/yr), respectively (Figure 5b, Table S2). From 2011-2016, these rates increased on SCB and NCB to 0.08 m/yr, with some locations growing by as much as 0.4 m/yr. While there was no net interannual change on SHB (0 m/yr), dune crests grew at an average rate of 0.02 m/yr to the east of km 4. Multi-kilometer stretches of the coast showed faster rates of dune accretion including transects located between kms 12-22 on NCB where crests increased from 0.03 m/yr (decadal) to 0.11 m/yr (interannual).

4.3 Time and Space Varying Beach and Foredune Morphology

The dune crest elevations (relative to the North American Vertical Datum 1988; NAVD88) and cross-shore dune toe location (relative to the 1997 dune toe position) were extracted at 40 m alongshore resolution from each of the ten lidar datasets (Table S1) across the study site (Figure 6). There were distinct regions where dune crest elevations were consistently high (e.g., near the alongshore distance at km 5 on SHB

and km 13 on SHB and SCB) and low (e.g., km 25 on NCB) across the nearly two decades (Figure 6a). Apart from Power Squadron Spit on SCB (kms 0-5), which was largely accretional, dunes tended to be lower on the ends of the islands near inlets, including the eastern and western ends of SHB and the northern extents of SCB and NCB (Figure 6a). In some instances, including the western end of SHB, these regions eroded to the point of no longer having distinguishable dune features and expanded in the lateral direction over time. The opening, closing, and migration of New-Old Drum Inlet around km 5 on NCB and the development of a large overwash fan near km 32 on NCB was also evident (Figure 1, Figure 6a).

The central regions on the islands (i.e., between kms 4-14 on SHB, kms 8-36 on SCB, and kms 7-27 on NCB) showed both accretion and erosion (Figure 6a). The lidar datasets from 2001 and 2004 captured extensive lowering of the dune crest heights, especially along SCB (-0.6 m) and NCB (-1.02 m). Dunes recovered from 2004-2005 along the aforementioned areas by 0.04 m and 0.2 m, respectively, but remained in a generally lowered state. The dune crest heights in 2011 compared to those in 2005 indicate that the dune response was variable during this time; average recovery on SCB and NCB was 0.10 m and 0.32 m, respectively. The eastern side of SHB (kms 4-7) eroded by 0.61 m while the western side (kms 7-14) recovered by 0.29 m (Figure 6a).

Generally, since 1997, the cross-shore position of the dune toes retreated over time across all three islands (Figure 6b). The average retreat of the dune toe location in 2016

for SHB, SCB, and NCB was -42.1, -31.5, and -17.9 m, respectively. Prior to 2011, retreat occurred at 75%, 70%, and 77% of the dunes on SHB, SCB, and NCB, respectively. In more recent years, 2011-2016, retreat increased to 84%, 84%, and 86% of dunes on SHB, SCB, and NCB. Progradation occurred on the eastern end of SHB, the northern tip of Power Squadron Spit on SCB (kms 0-3), near Cape Lookout Shoal (around km 5 on SCB), and between kms 29–33 on NCB (Figure 1, 6b). Dunes within these regions were generally shorter and, in many instances, progradation occurred where proto dunes were created and developed shoreward of existing dunes. Beginning in 2012, significant dune retreat occurred on the western end of SHB and the northernmost extents of SCB and NCB adjacent to inlets (Figure 6).

4.4 Foredune Erosion Potential

The number of collision and overwash hours per year varied considerably among the islands and over the study period (Figure 7). The average transect within CALO experienced 394 and 51 collision and overwash hours per year, respectively. Transects near the ends of the islands, particularly the eastern and western ends of SHB and the northern extents of SCB and NCB, experienced 2.3 times more collision and 4.2 times more overwash hours per year than the average CALO transect. Areas with lower TWL impact values tended to reside within the more central regions of the islands and along SCB's Power Squadron Spit (kms 0-5). Of these central areas (i.e., between kms 4-14 on SHB, kms 8-36 on SCB, and kms 7-27 on NCB) SHB had 1.4 and 1.3 times more

collision hours per year per transect than SCB and NCB from 1998-2017 while NCB had 1.5 and 2.4 times the number of overwash hours per year per transect compared to SHB and SCB.

Both relatively calm periods and years with more elevated TWL impacts were observed throughout the two decades (Figure 7). Between 2000-2002, less than an average of 28 hours per year of overwash occurred along each island. Impact hours peaked in 2003 and, in 2005, collision hours on SCB and NCB were 1.3 and 1.2 times above the average number of collision hours per transect for their respective islands (Figure 7a). This was followed by a period of sustained, higher impact hours across all islands from 2006-2011. Widespread overwash occurred along CALO in 2011 when 70% of SHB, 75% of SCB, and 76% of NCB dunes experienced at least one hour of overtopping. After 2013, impact hours on SCB and NCB were relatively limited and steady, particularly for more centrally located regions, whereas SHB experienced more variability from year to year (Figure 7).

The TWL analysis showed the following storms produced the five largest TWLs, in descending order, throughout the study site: Bonnie (1998), Isabel (2003), Irene (2011), Floyd (1999), and Dennis (1999) (Table 1). Additionally, 15 out of the 23 storms listed in Table 1 were associated with one of the five largest TWL events per year (i.e., total 100 TWL events from 1997-2017 at each transect). Over 90% of the transects within the study site connected storms Bonnie (1998), Isabel (2003), Irene (2011), Floyd (1999),

Dennis (1999), and Ophelia (2005) with one of the five largest annual TWL events. The highest frequency of significant storms occurred in 1999, when Tropical Storm Dennis and Hurricanes Floyd and Irene impacted the region within a single year.

4.5 Foredune Accretion Potential

The spatial distribution of dune building hours per year was largely dependent on the shoreline orientation, which affects the cross-shore wind component (Figure 8). Power Squadron Spit on SCB and SHB are exposed to southwest winds, which is the dominant wind direction (Figure 2), and as a result, these two reaches of coast had the greatest number of dune building hours per year (more than 350 hours per transect) while the east facing shorelines of SCB and NCB typically had fewer than 200 hours per year (Figure 8). Smaller scale variation was also evident. Km 13 on SHB consistently experienced over 300 dune building hours per year per transect over the nearly two decades while km 32 on NCB where the overwash fan developed, had typically less than 50 hours per year.

The temporal variation of the annual dune building hours per year were more similar among SCB and NCB compared to SHB (Figure 8). Dune building potential peaked on SCB and NCB in 1998, 1999, 2002, and 2011 and on SHB in 1999, 2000, 2003, and 2011. Dune building hours in 2011 for SHB, SCB, and NCB were 1.4, 1.3, and 1.3 times the average hours per year per transect. Years with high accretion potential were often followed by a gradual decline in dune building hours in subsequent years. After 2013,

dune building hours were high between kms 18-29 on NCB and this pattern continued westward in 2014-2015. The average dune building hours per year on SHB decreased over the past two decades, but they remained the same (within the range of 100-250 hours) on SCB and NCB.

4.6 Net Effect of Foredune Accretion and Erosion Potential

The constructive-destructive dune forcing (CDDF) ratio quantifies the net effect of foredune accretion and erosion potential. The CDDF ratio was positive (more accretion potential) 52% of the time from 1998-2017 and negative (more erosion potential) 48% of the time (Figure 9). Throughout the study period, most transects were in a dune building state more often than in an erosive condition. However, the strong negative to slightly positive values of the CDDF ratio, ranging from -60% to 10%, indicate that TWL impact hours significantly exceed dune building hours for particular transects and years. The average CDDF for SHB, NCB, and SCB was -1.7%, -2.5%, and -3.7%, respectively, signifying that the erosion potential was slightly greater than the accretion potential for all three islands. CDDF values were more negatively skewed on the east and west ends of SHB and on the northern ends of SCB and NCB. More centrally located dunes (i.e., kms 4-14 on SHB, kms 8-36 on SCB, and kms 7-27 on NCB) tended to have slightly negative values (e.g., -1.1%, -2.2%, and -2.1%, respectively) (Figure 9). Particular years, including 2005-2010 and 2012, also ranked higher in potential erosion. Larger, positive ratios occurred on the east/west oriented shorelines of SHB and Power

Squadron Spit on SCB, though accretion potential on SHB decreased from 3.6% between 1998-2004 to 1.5% between 2005-2016.

5 Discussion

Results of this study document how beaches and foredunes at Cape Lookout National Seashore, North Carolina, have changed at varying temporal and spatial scales using airborne lidar. In the following sections, we explore the possible causes of these changes by considering the relationships between constructive and destructive processes related to foredune evolution.

5.1 Relationships Between Constructive to Destructive Processes and Foredune Morphology

Dune crest elevations were inversely related to the collision and overwash regimes, which constitute the destructive forcing metric, and positively related to the dune building hours (constructive forcing metric; Figure 6; 7; 8). Lower dunes near the ends of the islands frequently experienced TWLs that reached or exceeded the dune toe and crest elevations. As a result, these areas were wet more often, resulting in smaller fetch lengths and reduced dune building hours. Even though South Core Banks (SCB) and North Core Banks (NCB) coastlines are more exposed to the dominant wave direction, Shackleford Banks (SHB) was estimated to have more collision hours per year, which was likely a product of the narrower beach widths and steeper beach slopes, resulting in

larger runup (Figure 2; 4; 7a). However east/west oriented shorelines, i.e., SHB and Power Squadron Spit on SCB, consistently had larger dunes compared to other regions of CALO. This is likely driven by the shoreline being exposed to the dominant, cross-shore wind direction, giving rise to a large number of dune building hours per year (Figure 8). NCB had the lowest dune crest elevations of the three islands and experienced the highest frequency of overwash (Figure 7b). The net gain in dune volume on NCB from 1997-2016 (Table S3) was likely due to a combination of sand deposition at the dune toe and crest, as well as on the leeward side of the dune during overwash events (Sallenger, 2000). Smaller spatial scale variations in the univariate metrics analyzed here are likely a product of local beach and dune morphology, particularly the beach width, foreshore slope, and dune toe elevation. For example, between kms 13-14 on SHB, beach widths were approximately 43% wider than the island average, and this area experienced few impact hours and a large number of dune building hours (approximately 200-350) each year throughout the nearly two decades of the study (Figure 6; 7; 8). This region also had dune crests that were 13% higher than the island average. In general, wide beach widths, shallower foreshore slopes, and higher dune toe and crests reduce impact hours due to decreased runup. TWL reduction increases dune building hours via greater fetch lengths and potentially increased number of consecutive hours the dune building criteria are met.

The CDDF ratio corroborates the spatial and temporal patterns seen in the individual TWL impact and dune building metrics. Erosion potential was higher in regions with low-lying dunes, e.g., northern extents of SCB and NCB, and accretion potential was higher in areas with large dunes, e.g., km 13 on SHB (Figure 9). The CDDF ratio estimated constructive processes driving interannual (2011-2016) foredune recovery (e.g., kms 12-22 on NCB), and the limited dune crest growth on SHB at the decadal scale (1997-2016; Section 4.1) may be explained by the average decline in accretion potential on this island. The CDDF ratio, however, failed to capture the destructive forces that led to significant erosion of the dunes between the 2001 and 2004 lidar datasets despite the widespread, high number of overwash hours predicted between those years. This lack of prediction indicates that 1) collision hours and overwash hours may need to be weighted differently instead of summed one to one in the TWL impact metric, 2) not all impact hours are created equal in terms of the effects on the morphology, even within a single impact regime, and/or 3) sub-interannual changes in beach and dune morphology are not adequately resolved by lidar and impact hours may be underestimated, or in the case of recovery, overestimated as a result.

5.2 Relative Importance of Constructive Versus Destructive Processes in Foredune Evolution

The correlation between the average dune toe and crest elevations and the number of TWL impact hours per year, dune building hours per year, and the CDDF ratio were

tested at three different spatial scales. We provide examples at a single transect located at km 5 on SHB, a two-kilometer-long region from kms 19-21 on SCB (50 transects), and a 20-kilometer span from kms 7-27 on NCB (500 transects). Additionally, the minimum and maximum correlation of all individual transects on SHB and two-kilometer-long sections on SCB were calculated to provide context for how the examples shown herein compare to other locations at these spatial extents (Table 2; grey values). At all three spatial scales, the dune toe elevation showed an inverse relationship with the average number of TWL impact hours per year, explaining 45%-51% of the variance in this morphometric (Figure 10; Table 2). Fluctuations in the dune toe elevation mirrored the average number of dune building days for the single transect at km 5 on SHB, where taller dune toe elevations were associated with a greater number of potential dune building hours (Figure 10a). The average number of dune building hours was more variable for the two-kilometer (kms 19-21 on SCB) and 20-kilometer (kms 7-27 on NCB) examples, and the correlation with the dune toe elevation was not statistically significant. However, other examples along SCB where two-kilometer sections were averaged, showed the R^2 values at the 95% confidence level ranged from 0.21-0.56 (Table 2; grey values). The decrease in correlation between the dune building hours per year and dune toe elevation as the spatial averaging increased from single to two-kilometers to 20-kilometers implies that averaging at larger spatial scales may oversimplify constructive responses (Table 2). At the single transect scale, the CDDF

ratio explained 75% of the variance in the dune toe elevation, which was superior to its components, i.e., only 51% of the variance was explained by impact hours alone and only 63% by dune building hours alone. However, an increase in dune toe elevation did not always coincide with a positive, constructive CDDF value. For example, the CDDF values at kms 19-21 on SCB tended to be more negatively skewed, even when the dune toe accreted. This suggests that in the absence of statistically significant dune building hours, the value of the CDDF ratio may be negatively skewed. Regardless, the correlation coefficients for the TWL impact hours per year were analogous to those of the CDDF ratio, indicating that changes in dune toe elevations were primarily explained by TWL impacts rather than dune building processes at multiple spatial scales. For applications that require multi-kilometers spatial averaging, TWL impact hours, as opposed to building hours, will be most effective at estimating dune toe elevations.

Dune crest elevations were also inversely related to impact hours per year (Figure 11). The correlations were not significant for dune building hours for any of the three examples suggesting (1) parameters used in calculating dune building hours per year, such as the threshold velocity or critical fetch length, may need to be adjusted, and/or (2) other processes that contribute to changes in the dune crest elevation are not accounted for in our metrics (Table 2). The CDDF ratio was positively correlated to the dune crest elevation for the SCB and NCB examples and had good agreement during both erosional and accretional behavior of the dune crest (Figure 11b, c). TWL impact

hours, dune building hours, and the CDDF ratio were not significantly correlated to the dune crest elevation at km 5 on SHB. However, these metrics showed general agreement with the dune crest change at this location, despite the beach state captured by the lidar datasets and intermittent lidar acquisition. For example, the 2005 lidar dataset was collected following Hurricane Ophelia, thus it represented a more eroded beach state. Beach and dune morphology were held constant for the metric calculations until the 2011 lidar dataset was acquired. At km 5 on SHB, between 2005 and 2011, TWL impact hours increased, dune building hours reduced, the CDDF ratio was estimated to be in a destructive state; additionally, the dune crest elevation lowered approximately 1 m from 2005 to 2011 (Figure 11a). The general behavior of these univariate metrics during this period indicates they may be used to approximate changes in dune crest elevations despite a range of beach slope variability for upwards of five years in the absence of interannual lidar collection.

The percent of transects between kms 4-14 on SHB, kms 8-36 on SCB, and kms 7-27 on NCB that had significant correlations between dune toe elevation and the TWL impact hours per year, dune building hours per year, and CDDF ratio were 61%, 58%, and 69%, respectively (Table 2). Dune morphometric changes averaged at larger spatial scales can be primarily explained by impact hours per year. However, when both the constructive and destructive forces are adequately captured, they bolster the correlative power of the CDDF ratio. Additionally, of the three metrics that were

assessed at the single transect scale across kms 4-14 on SHB, kms 8-36 on SCB, and kms 7-27 on NCB, the CDDF ratio explained the highest percentage of variance in dune toe and crest elevation.

5.3 Response to Storm Events and Recovery

The six most impactful storms for CALO from 1997-2016 based on the TWL analysis were: Bonnie (1998), Floyd (1999), Dennis (1999), Isabel (2003), Ophelia (2005), Irene (2011) (in sequential order; Table 1; Section 4.4). The morphologic, constructive, and destructive forcing metrics' response to these storms was dependent on several factors including storm frequency, proximity, pre-existing morphology, and shoreline orientation (Figure 6; 7; 8). Hurricane Bonnie (1998) made landfall southwest of CALO near Wilmington, NC, followed by Tropical Storm Dennis and Hurricane Floyd in 1999. The 1998 and 1999 lidar datasets (flown prior to Hurricane Irene, 1999) show SHB, which was the closest in proximity to Bonnie and Floyd, experienced the greatest number of TWL impact hours, dune erosion (-0.1 m), and dune retreat (-5 m) of all three islands. NCB had comparatively less TWL impact hours and a high number of dune building hours, exceeded 250, suggesting that moderate exposure to storms based on proximity and shoreline orientation may promote constructive processes.

Several storms impacted the region between 2001 and 2004 (Table 1). The high frequency of storms during this time make it difficult to attribute morphological change to any one event, however extensive erosion and retreat occurred within the study site.

Hurricane Isabel (2003) produced TWLs as large as 10.3 m (NAVD88) and over 97% of the transects within CALO identified this storm as one of the five largest annual TWL events (Table 1). Closest in proximity to Isabel's landfall, NCB experienced the greatest erosion (-0.91 m), retreat (-33.5 m), and the highest number of TWL impact hours per year from 2001-2004, which peaked in 2003. The estimated TWL impact hours were also high in 2005; despite this, dune crests elevation increased from 2004 to 2005 (Figure 9). This accretion may have been precipitated by Hurricane Ophelia in 2005, which stayed off the coast of the Outer Banks and produced moderate TWLs and high winds, possibly resulting in aeolian and/or marine driven sediment transport to the dunes (Cohn et al., 2019b).

In 2011, Hurricane Irene made landfall near Cape Lookout and produced some of the most elevated TWLs and widespread overtopping across all three islands. Although Irene eroded dunes along CALO (e.g., kms 3-7 on SHB, kms 28-38 on SCB, and kms 5-10 on NCB), many regions (e.g., kms 9-14 on SHB, km 4 and kms 9-25 on SCB, and kms 11-29 on NCB) are speculated to have been in a state of recovery prior to 2011, and therefore more resilient to Irene's impacts. Between 2011 and 2016, SCB and NCB generally recovered despite the relatively high frequency of storms events, most of which produced only moderate TWLs. Dunes on NCB rapidly rebounded, growing 0.3 m from 2011-2012 whereas the rate on SCB was about half that. These two islands recovered at rates between 0.01-0.12 m/yr from 2012 to 2016.

5.4 Limitations and Relevance

In this paper, we use lidar extracted beach and dune morphology to quantify the evolution of barrier island dunes and assess the constructive and destructive processes that drive these morphometric changes. However, these results are bound by the timing and frequency of lidar acquisition, which may cause a higher number of deviations in predicted TWL impact and dune building hours that are not a direct result of forcing conditions (e.g., elevated TWL), but rather, reflect the beach and dune state (i.e., post-storm conditions versus recovered) at the time of lidar acquisition. One such example is the elevated impact hours from 2005-2011. This may be an artifact of a lowered beach state caused by Hurricane Ophelia (2005), which was captured in the 2005 lidar dataset and held constant through 2011 for the TWL analysis. While the general behavior of the univariate metrics may be used to infer dune changes (Section 5.2), the extent of natural dune recovery processes may not be captured adequately by the constructive and destructive metrics, and more uncertainty is introduced as the time between lidar collection increases.

Application of the stationary still water level and the wave filtering approach to address sheltering effects due to varying shoreline orientations may smooth or distort the variability of the alongshore TWLs, ultimately altering the number of estimated impact and dune building hours. High fidelity models that incorporate spatial variability in physical processes such as storm surge, wave refraction, and nearshore morphology

change may provide a better avenue to estimate the TWLs needed for our metrics. Additionally, other controls that have been shown in the literature to affect dune growth, stability, and recovery that have not been incorporated here include sediment budget (e.g., Davidson-Arnott et al., 2018; Jay et al., in revision.; Psuty, 1988), sediment characteristics (e.g., sorting and armoring and surface moisture; Belly, 1964; Davidson-Arnott et al., 2005; de Vries et al., 2014), wave driven sediment transport (e.g, Cohn et al., 2019b; Houser and Hamilton, 2009), and vegetation characteristics (e.g., Arens et al., 2001; Biel et al., 2019; Charbonneau et al., 2017; Durán and Moore, 2013; Godfrey, 1977, 1976; Goldstein et al., 2017; Hacker et al., 2019, 2012; Hesp, 1989; Mullins et al., 2019; Reijers et al., 2019; Seabloom et al., 2013; Wolner et al., 2013; Zarnetske et al., 2012). Recently developed, state-of-the-art models that simulate the co-evolution of beach and dune systems may also provide a more controlled way to explore how dune systems respond to these factors, and is a focus of ongoing research (Cohn et al., 2019a; Larson et al., 2016; Roelvink and Costas, 2019).

This research incorporates and expands upon concepts previously explored in the literature including the use of TWL impact hours per year as a proxy for erosion of foredunes (e.g., Ruggiero et al., 2001; Wahl et al., 2016; Wahl and Plant, 2015) and the work of Delgado-Fernandez and Davidson-Arnott (2011) for establishing dune building criteria. We collapse constructive and destructive processes related to foredune evolution into simplified metrics to better understand changes in foredune morphology.

This approach diverges from more stylized, conceptual models (e.g., Psuty, 1988; Short and Hesp, 1982) as well as complex, process-based, numerical models (e.g., (Cohn et al., 2019a; Roelvink and Costas, 2019) towards a simply, yet quantitative, multi-spatial, multi-temporal approach that incorporates both constructive and destructive processes. The simplicity of these metrics supports versatility in applying these methods across multiple spatial scales (i.e., single transect to tens of kilometers) and temporal scales (i.e., annual to decadal) and for this reason may provide a robust first order estimate of dune evolution across highly variable coastlines, particularly where lidar acquisition is intermittent. Utilizing publicly available datasets from buoys, meteorological stations, and model hindcasts /forecasts, this approach is readily employable for locations where these data exist. In practice, these metrics may be used as standalone products to quantify accretional and erosional processes on any dune backed coastline. They may also be applied within the scope of other predictive frameworks to improve estimates of present-day morphology and enhance operational forecasts of storm impacts (e.g., USGS Coastal Change Hazards forecasts; USGS, 2021) and coastal vulnerability estimates for management decisions (e.g., Mills et al., 2018). Further, the simplicity of these metrics allows them to be easily supplemented by additional resources (i.e., outputs from statistical or numerical models) and adapted to incorporate more complex processes (e.g., marine driven sediment transport, ecomorphodynamic processes) and management scenarios (e.g., beach nourishment, dune grading),

6 Conclusions

Beach and dune morphometrics were extracted from ten lidar datasets from 1997-2016 at 40 m alongshore resolution across Cape Lookout National Seashore, North Carolina. Since 1997, dune toe locations on all three islands have generally retreated. However, despite frequent storms in this region that have caused localized and extensive dune erosion, dune crests have, on average, accreted at both the decadal and interannual scale, with larger and more variable rates from 2011-2016. Rapid changes from one lidar dataset to the next indicates that the frequency at which lidar is collected under-samples the natural changes that are occurring.

Simple univariate metrics of total water level (TWL) impact hours per year, dune building hours per year, and a relative constructive-destructive dune forcing (CDDF) ratio were developed using open-source wave hindcasts and wind data to explain dune morphometric changes over varying spatial and temporal scales. These metrics provide a versatile approach to infer foredune morphology between coastal mapping campaigns, which may occur at irregular intervals and be costly or logistically complex to collect. Better prediction of coastal change has implications for improved coastal hazard forecasts and management decision making at spatial scales ranging from a single, cross-shore transect to multi-kilometers stretches of coast. The TWL impact hours per year and CDDF metric explain variations in dune toe and crest elevation and may be helpful for estimating interannual changes in the absence of lidar collection.

Greater constructive forces are estimated for regions exposed to the dominant cross-shore wind direction and relatively narrow beach widths, suggesting fetch is not the dominant limiting driver to constructive processes within our study. Taken together, we show that these three univariate metrics, which use a simplified approach to capture complex constructive and destructive processes, may be used to better understand the alongshore variability and temporal change of coastal foredunes.

Conflict of Interest Statement

The authors declare that there is no conflict of interest.

References

Arens, S.M., Baas, A.C.W., Boxel, J.H. Van, Kalkman, C., 2001. Influence of Reed Stem Density on Foredune Development. Earth Surf. Process. Landforms 26, 1161–1176. https://doi.org/10.1002/esp.257

Bagnold, R.A., 1941. The Physics of Blown Sand and Desert Dunes. Methuen, London.

Barbier, E.B., Hacker, S.D., Kennedy, C., Koch, E.W., Stier, A.C., Silliman, B.R., 2011. The value of estuarine and coastal ecosystem services. Ecol. Monogr. 81, 169–193. https://doi.org/10.1890/10-1510.1

Bauer, B.O., Davidson-Arnott, R.G.D., 2003. A general framework for modeling sediment supply to coastal dunes including wind angle, beach geometry, and fetch effects. Geomorphology 49, 89–108.

Bauer, B.O., Davidson-Arnott, R.G.D., Hesp, P.A., Namikas, S.L., Ollerhead, J., Walker, I.J., 2009. Aeolian sediment transport on a beach: Surface moisture, wind fetch, and mean transport. Geomorphology 105, 106–116.

Belly, P.Y., 1964. Sand Movement by Wind. Washington DC.

Beuzen, T., 2019. pybeach : A Python package for extracting the location of dune toes on beach profile transects. J. Open Source Softw. 4, 1890. https://doi.org/10.21105/joss.01890

Biel, R.G., Hacker, S.D., Ruggiero, P., 2019. Elucidating Coastal Foredune Ecomorphodynamics in the U.S. Pacific Northwest via Bayesian Networks. J. Geophys. Res. Earth Surf. 124, 1919–1938. https://doi.org/10.1029/2018JF004758

Charbonneau, B.R., Wooton, L.S., Wnek, J.P., Langley, J.A., Posner, M.A., 2017. A species effect on storm erosion: Invasive sedge stabilized dunes more than native grass during Hurricane Sandy. J. Appl. Ecol. 54, 1385–1394. https://doi.org/10.1111/1365-2664.12846

Cohn, N., Hoonhout, B., Goldstein, E., De Vries, S., Moore, L., Durán Vinent, O., Ruggiero, P., 2019a. Exploring Marine and Aeolian Controls on Coastal Foredune Growth Using a Coupled Numerical Model. J. Mar. Sci. Eng. 7, 13. https://doi.org/10.3390/jmse7010013

Cohn, N., Ruggiero, P., Garcia-Medina, G., Anderson, D., Serafin, K.A., Biel, R.G., 2019b. Environmental and morphologic controls on wave-induced dune response.

Geomorphology 329, 108–128.

Davidson-Arnott, R., Hesp, P., Ollerhead, J., Walker, I., Bauer, B., Delgado-Fernandez, I., Smyth, T., 2018. Sediment budget controls on foredune height: Comparing simulation model results with field data. Earth Surf. Process. Landforms 43, 1798–1810. https://doi.org/10.1002/esp.4354

Davidson-Arnott, R., Law, M., 1990. Seasonal patterns and controls on sediment supply to coastal foredunes, Long Point, Lake Erie, in: Coastal Dunes: Form and Process. pp. 177–200.

Davidson-Arnott, R., MacQuarrie, K., Aagaard, T., 2005. The effect of wind gusts, moisture content and fetch length on sand transport on a beach. Geomorphology 68, 115–129.

de Vries, S., de Vries, J.S.M. van T., van Rijn, L.C., Arens, S.M., Ranasinghe, R., 2014. Aeolian sediment transport in supply limited situations. Aeolian Res. 12, 75–85. https://doi.org/10.1016/j.aeolia.2013.11.005

Delgado-Fernandez, I., 2010. A review of the application of the fetch effect to modelling sand supply to coastal foredunes. Aeolian Res. 2, 61–70.

Delgado-Fernandez, I., Davidson-Arnott, R., 2011. Meso-scale aeolian sediment input to coastal dunes : The nature of aeolian transport events. Geomorphology 126, 217–232. https://doi.org/10.1016/j.geomorph.2010.11.005

Dolan, R., Lins, H., 1985. The Outer Banks of North Carolina. Washington DC.

Durán, O., Moore, L.J., 2013. Vegetation controls on the maximum size of coastal dunes. PNAS 10, 17217–17222. https://doi.org/10.1073/pnas.1307580110

Durán Vinent, O., Moore, L.J., 2015. Barrier island bistability induced by biophysical interactions. Nat. Clim. Chang. 5, 158–162.

Elko, N.A., Sallenger, A.H., Guy, K., Stockdon, H.F., Morgan, K.L.M., Carolina, N., 2002. Barrier Island Elevations Relevant to Potential Storm Impacts : 1 . Techniques.

Fryberger, S.G., Dean, D., 1979. Dune forms and wind regime, in: Study of Global Sand Seas. U.S. Geological Survey, pp. 141–151.

Godfrey, P.J., 1977. Climate, plant response and development of dunes on barrier beaches along the U.S. east coast. Int J Biometeorol 21, 203–216. https://doi.org/10.1007/BF01552874

Godfrey, P.J., 1976. Barrier Island Ecology of Cape Lookout National Seashore and Vicinity, North Carolina. National Park Service.

Goldstein, E.B., Moore, L.J., 2016. Stability and bistability in a one-dimensional model of coastal foredune height. J. Geophys. Res. Earth Surf. 121, 964–977. https://doi.org/10.1002/2015JF003783

Goldstein, E.B., Moore, L.J., Vinent, O.D., 2017. Lateral vegetation growth rates exert control on coastal foredune " hummockiness " and coalescing time. Earth Surf. Dyn. 5, 417–427.

Hacker, S.D., Jay, K.R., Cohn, N., Goldstein, E.B., Hovenga, P.A., Itzkin, M., Moore, L.J., Mostow, R.S., Mullins, E. V, Ruggiero, P., 2019. Species-Specific Functional Morphology of Four US Atlantic Coast Dune Grasses : Biogeographic Implications for Dune Shape and Coastal Protection. Diversity 11, 82.

Hacker, S.D., Zarnetske, P., Seabloom, E., Ruggiero, P., Mull, J., Gerrity, S., Jones, C., 2012. Subtle differences in two non-native congeneric beach grasses significantly affect their colonization, spread, and impact. Oikos 121, 138–148. https://doi.org/10.1111/j.1600-0706.2011.18887.x

Hallin, C., Larson, M., Hanson, H., 2019. Simulating beach and dune evolution at decadal to centennial scale under rising sea levels. PLoS One 14, 1-30r. https://doi.org/10.1371/journal.pone.0215651

Halls, J.N., Frishman, M.A., Hawkes, A.D., 2018. An automated model to classify barrier island geomorphology using lidar data and change analysis (1998-2014). Remote Sens. 10, 1–21. https://doi.org/10.3390/rs10071109

Hesp, P.A., 1989. A review of biological and geomorphological processes involved in the initiation and development of incipient foredunes. Proc. R. Soc. Edinburgh, Sect. B Biol. Sci. 96, 181–201.

Hoonhout, B.M., Vries, S. de, 2016. A process-based model for aeolian sediment transport and spatiotemporal varying sediment availability. J. Geophys. Res. Earth Surf. 121, 1555–1575. https://doi.org/10.1002/2015JF003692

Hosier, P.E., Cleary, W.J., 1977. Cyclic geomorphic patterns of washover on a barrier Island in southeastern North Carolina. Environ. Geol. 2, 23–31. https://doi.org/10.1007/BF02430662

Houser, C., 2009. Synchronization of transport and supply in beach-dune interaction. Prog. Phys. Geogr. 33, 733–746. https://doi.org/10.1177/0309133309350120

Houser, C., Hamilton, S., 2009. Sensitivity of post-hurricane beach and dune recovery to event frequencyle. Earth Surf. Process. Landforms 34, 613–628.

Hovenga, P.A., Ruggiero, P., Cohn, N., Jay, K.R., Hacker, S.D., Itzkin, M., Moore, L.J., 2019. Drivers of Dune Evolution in Cape Lookout National Seashore, Nc, in: Coastal Sediments 2019. pp. 1283–1296. https://doi.org/10.1142/9789811204487_0112

Jay, K.R., Hacker, S.D., Hovenga, P.A., Moore, L.J., Ruggiero, P., n.d. Sand supply and dune grass species affect foredune shape along the US Central Atlantic Coast. Ecology.

Keijsers, J.G.S., Groot, A.V. De, Riksen, M.J.P.M., 2016. Earth Surface Modeling the biogeomorphic evolution of coastal dunes. J. Geophys. Res. Earth Surf. 121, 1161–1181. https://doi.org/10.1002/2015JF003815.Abstract

Klemas, V., 2011. Beach Profiling and LIDAR Bathymetry: An Overview with Case Studies. J. Coast. Res. 27, 1019–1028. https://doi.org/10.2112/JCOASTRES-D-11-00017.1

Larson, M., Palalane, J., Fredriksson, C., Hanson, H., 2016. Simulating cross-shore material exchange at decadal scale. Theory and model component validation. Coast. Eng. 116, 57–66. https://doi.org/10.1016/j.coastaleng.2016.05.009

Lettau, K., Lettau, H., 1977. Experimental and micrometeorological field studies of dune migration.

Lynch, K., Jackson, D.W.T., Andrew, J., Cooper, A.G., 2008. Aeolian fetch distance and secondary airflow effects : the influence of micro-scale variables on meso-scale foredune development. Earth Surf. Process. Landforms 33, 991–1005. https://doi.org/10.1002/esp

Mallinson, D., Culver, S., Riggs, S., Walsh, J., Ames, D., Smith, C., 2008. Past , Present and Future Inlets of the Outer Banks Barrier Islands, North Carolina. East Carolina University Printing Press, Greenville.

Mills, A.K., Bolte, J.P., Ruggiero, P., Sera, K.A., Lipiec, E., Corcoran, P., Stevenson, J., Zanocco, C., Lach, D., 2018. Exploring the impacts of climate and policy changes on coastal community resilience : Simulating alternative future scenarios. Environ. Model. Softw. 109, 80–92. https://doi.org/10.1016/j.envsoft.2018.07.022

Mitasova, H., Overton, M.F., Recalde, J.J., Bernstein, D.J., Freeman, C.W., 2009. Raster-Based Analysis of Coastal Terrain Dynamics from Multitemporal Lidar Data. J. Coast. Res. 25, 507–514. https://doi.org/10.2112/07-0976.1

Moore, L., Durán Vinent, O., Ruggiero, P., 2016. Vegetation control allows autocyclic

formation of multiple dunes on prograding coasts. Geology 44, 559–562. https://doi.org/10.1130/G37778.1

Mull, J., Ruggiero, P., 2014. Estimating Storm-Induced Dune Erosion and Overtopping along U . S . West Coast Beaches Estimating Storm-Induced Dune Erosion and Overtopping along U . S . West Coast Beaches. J. Coast. Res. 30, 1173–1187. https://doi.org/10.2112/JCOASTRES-D-13-00178.1

Mullins, E., Moore, L.J., Goldstein, E.B., Jass, T., Bruno, J., Vinent, O.D., 2019. Investigating dune-building feedback at the plant level: Insights from a multispecies field experiment. Earth Surf. Process. Landforms 44, 1734–1747. https://doi.org/10.1002/esp.4607

NOAA Digital Coast, 2018. Historical Hurricane Tracks [WWW Document]. URL https://coast.noaa.gov/hurricanes/

NOAA Digital Coast, 2016. Data Access Viewer [WWW Document]. URL https://coast.noaa.gov/dataviewer/#/lidar/search/

Nordstrom, K.F., Jackson, N.L., 1992. Effect of source width and tidal elevation changes on aeolian transport on an estuarine beach. Sedimentology 39, 769–778.

Park, J.-Y., Wells, J.T., 2005. Longshore Transport at Cape Lookout, North Carolina: Shoal Evolution and the Regional Sediment Budget. J. Coast. Res. 211, 1–17. https://doi.org/10.2112/02051.1

Psuty, N.P., 1988. SEDIMENT BUDGET AND DUNE / BEACH. J. Coast. Res. 1–4.

Reijers, V.C., Siteur, K., Hoeks, S., Belzen, J. Van, Borst, A.C.W., Heusinkveld, J.H.T., Govers, L.L., Bouma, T.J., Lamers, L.P.M., van de Koppel, J., van der Heide, T., 2019. A Lévy expansion strategy optimizes early dune building by beach grasses. Nat. Commun. 10, 1–9. https://doi.org/10.1038/s41467-019-10699-8

Renaissance Computing Institute, n.d. ADCIRC NC6B Mesh.

Riggs, S.R., Ames, D. V, Culver, S., Mallison, D.J., 2011. The battle for North Carolina's coast. The University of North Carolina Press.

Ritchie, W., Penland, S., 1988. Cyclical Changes in the Coastal Dunes of Southern Louisiana. J. Coast. Res. Spec. Issue 111–114.

Roelvink, D., Costas, S., 2019. Coupling nearshore and aeolian processes: XBeach and duna process-based models. Environ. Model. Softw. 115, 98–112. https://doi.org/10.1016/j.envsoft.2019.02.010

Ruggiero, P., Kratzmann, M.G., Himmelstoss, E.A., Reid, D., Allan, J., Kaminsky, G., 2013. National Assessment of Shoreline Change : Historical Shoreline Change Along the Pacific Northwest Coast.

Ruggiero, P., Cohn, N., Hoonhout, B., Goldstein, E., de Vries, S., Moore, L., Hacker, S.D., Durán Vinent, O., 2019. Simulating dune evolution on managed coastlines: Exploring management options with the Coastal Recovery from Storms Tool (CReST). Shore and Beach 87, 36–43.

Ruggiero, P., Hacker, S., Seabloom, E., Zarnetske, P., 2018. The role of vegetation in

determining dune morphology, exposure to sea-level rise, and storm-induced coastal hazards: A U.S. Pacific Northwest perspective, in: Moore, L., Murray, A. (Eds.), Barrier Dynamics and Response to Changing Climate. Springer International Publishing AG 2018, pp. 337–361. https://doi.org/10.1007/978-3-319-68086-6_11

Ruggiero, P., Komar, P.D., McDougal, W.G., Marra, J.J., Beach, R.A., 2001. Wave Runup , Extreme Water Levels and the Erosion of Properties Backing Beaches. J. Coast. Res. 17, 407–419.

Sallenger, A., Stockdon, H., Fauver, L., Hansen, M., Thompson, D., Wright, C., Lillycrop, J., 2006. Hurricanes 2004 : An Overview of Their Characteristics and Coastal Change. Estuaries and coasts 29, 880–888.

Sallenger, A.H., 2000. Storm Impact Scale for Barrier Islands. J. Coast. Res. 16, 890–895. https://doi.org/10.2307/4300099

Seabloom, E.W., Ruggiero, P., Hacker, S.D., Mull, J., Zarnetske, P., 2013. Invasive grasses, climate change, and exposure to storm-wave overtopping in coastal dune ecosystems. Glob. Chang. Biol. 19, 824–832. https://doi.org/10.1111/gcb.12078

Sherman, D.J., Bauer, B.O., 1993. Dynamics of beach-dune systems. Prog. Phys. Geogr. 17, 413–447.

Short, A.D., Hesp, P.A., 1982. Wave, beach and dune interactions in southeastern Australia. Mar. Geol. 48, 259–284. https://doi.org/10.1016/0025-3227(82)90100-1

Spurgeon, J., 1999. The Socio-Economic Costs and Benefits of Coastal Habitat Rehabilitation and Creation. Mar. Pollut. Bull. 37, 373–382. https://doi.org/10.1016/S0025-326X(99)00074-0

Stockdon, H.F., Doran, K.S., Jr, A.H.S., Stockdon, H.F., Doran, K.S., Sallenger, A.H., 2009. Extraction of Lidar-Based Dune-Crest Elevations for Use in Examining the Vulnerability of Beaches to Inundation During Hurricanes Extraction of Lidar-Based Dune-Crest Elevations for Use in Examining the Vulnerability of Beaches to Inundation During Hurric. J. Coast. Res. SI, 59–65. https://doi.org/10.2112/SI53-007.1

Svasek, J., Terwindt, J., 1974. Measurements of sand transport by wind on a natural beach. Sedimentology 21, 311–312.

U.S. Army Corps. of Engineers, 1997. Available WIS Stations - Atlantic.

USGS, 2021. Coastal Change Hazards Portal [WWW Document]. URL https://marine.usgs.gov/coastalchangehazardsportal/

Wahl, T., Plant, N.G., 2015. Changes in erosion and flooding risk due to long-term and cyclic oceanographic trends. Geophys. Res. Lett. 2943–2950. https://doi.org/10.1002/2015GL063876

Wahl, T., Plant, N.G., Long, J.W., 2016. Probabilistic assessment of erosion and flooding risk in the northern Gulf of Mexico. J. Geophys. Res. Ocean. 121, 3029–3043. https://doi.org/10.1002/2015JC011482

Walker, I.J., 2020. Aeolian (windblown) sand transport over beaches, in: Sandy Beach Morphodynamics. Elsevier, pp. 213–253.

Wells, J.T., 1988. Accumulation of Fine-Grained Sediments in a Periodically Energetic Clastic Environment, Cape Lookout Bight, North Carolina. J. Sediment. Petrol. 58, 596–606. https://doi.org/10.1306/212f8dff-2b24-11d7-8648000102c1865d

Wolner, C.W. V, Moore, L.J., Young, D.R., Brantley, S.T., Bissett, S.N., Mcbride, R.A., 2013. Ecomorphodynamic feedbacks and barrier island response to disturbance : Insights from the Virginia Barrier Islands, Mid-Atlantic Bight, USA. Geomorphology 199, 115–128. https://doi.org/10.1016/j.geomorph.2013.03.035

Zarnetske, P.L., Hacker, S.D., Seabloom, E.W., Ruggiero, P., Killian, J.R., Maddux, T.B., Cox, D., 2012. Biophysical feedback mediates effects of invasive grasses on coastal dune shape. Ecology 93, 1439–1450.

Figure Captions

Figure 1. The study region including Shackleford Banks (SHB), South Core Banks (SCB), and North Core Banks (NCB), North Carolina, USA, which comprise the Cape Lookout National Seashore (CALO). Crosshairs, +, represent along-island distances in kilometers (kms).

Figure 2. Nearshore bathymetry from the Advanced CIRCulation NC6B mesh (Renaissance Computing Institute, n.d.) and locations of the observed NOAA 8656483 tide gauge (black square), Wave Information Studies (WIS) stations (black dots), and observed NOAA CLKN7 wind station (black star) are shown in the top figure. Wave height and direction from three WIS stations (top row) from 1997-2017 and wind speed and direction from the observed NOAA CLKN7 weather station and two WIS stations are shown in the bottom row.

Figure 3. Beach and dune morphometrics extracted from airborne lidar (figure modified from Mull and Ruggiero, 2014).

Figure 4. The probability density of the a) dune crest elevation b) dune toe elevation c) partial dune volume d) dune face slope, e) total dune volume, f) beach width, g) backshore slope, and h) foreshore slope for Shackleford Banks (SHB), South Core Banks (SCB), and North Core Banks (NCB), North Carolina, USA. Solid lines represent the probability density from all ten lidar datasets. Dotted lines and dashed lines are the probability density from the 1997 and 2016 lidar datasets, respectively. The x-axis limits represent data within ± two standard deviations about the mean of all three islands for each of the beach and dune metrics.

Figure 5. Alongshore varying decadal (1997-2016) and interannual (2011-2016) change rates of the a) foredune toe cross-shore positions and b) foredune crest elevations extracted from lidar for Shackleford Banks (SHB), South Core Banks (SCB), and North Core Banks (NCB), North Carolina, USA. Colored +

markers correspond with the along-island distances shown in Figure 1. Dots represent the raw data and solid lines are the smoothed data using a loess filter to remove signals shorter than 800 m.

Figure 6. Alongshore varying a) foredune crest elevations (m, NAVD88) (top) for Shackleford Banks (SHB; left panel), South Core Banks (SCB; middle panel), and North Core Banks (NCB; right panel) and b) foredune toe locations relative to the 1997 position (m). Years in red text indicate when a new lidar dataset was collected. Colored + markers correspond with along-island distances shown in Figure 1. Grey regions represent years when lidar data was not collected or locations of erroneous data (e.g., noisy cross-shore profiles where coherent beach and dune features could not be identified). The color bar axis limits represent ± two standard deviations about the mean for all data points within the CALO study domain.

Figure 7. Hours per year (hpy) spent in the a) collision and b) overwash regimes for Shackleford Banks (SHB; left panel), South Core Banks (SCB; middle panel), and North Core Banks (NCB; right panel), North Carolina, USA. Years in red text indicate when a new lidar dataset was collected. The color bar limits show the number of collision and overwash hpy within the 90^{th} percentile of the cumulative distribution. Note that the range of the color bar is different for the two plots. Grey regions represent locations where all beach and dune morphometrics required for the TWL calculations could not be identified.

Figure 8. Dune building hours per year (hpy) for Shackleford Banks (SHB; left panel), South Core Banks (SCB; middle panel), and North Core Banks (NCB; right panel), North Carolina, USA. Years in red text indicate when a new lidar dataset was collected. The color bar limits show data within the 90^{th} percentile of the cumulative distribution. Grey regions represent locations where all beach and dune morphometrics required for the TWL calculations could not be identified, and therefore, dune building hours could not be calculated.

Figure 9. Percent of constructive to destructive dune forcing (CDDF) for each year along Shackleford Banks (SHB; left panel), South Core Banks (SCB; middle panel), and North Core Banks (NCB; right panel), North Carolina, USA. Years in red text indicate when a new lidar dataset was collected. Positive values (cool colors) represent net constructive dune forcing, i.e., more dune building than TWL impact hours. Negative values (warm colors) represent net destructive dune forcing, i.e., more impact than dune building hours. Grey regions represent locations where all beach and dune morphometrics required for the TWL impact and dune building calculations could not be identified.

Figure 10. The spatially averaged impact hpy (left column), dune building hpy (middle column), and CDDF percent (right column) compared to the spatially averaged dune toe elevation, m (NAVD88), for a) a single transect at km 5 on Shackleford Banks (SHB), b) a two-kilometer region (50 transects) between kms 19-21 on South Core Banks (SCB), and c) a 20-kilometer area (500 transects) between kms 7-27 on North Core Banks (NCB). Black dots on the dune toe elevation plots represent years when new lidar was collected.

Figure 11. The spatially averaged impact hpy (left column), dune building hpy (middle column), and CDDF percent (right column) compared to the spatially averaged dune crest elevation, m (NAVD88), for a) a single transect at km 5 on Shackleford Banks (SHB), b) a two-kilometer region (50 transects) between kms 19-21 on South Core Banks (SCB), and c) a 20-kilometer area (500 transects) between kms 7-27 on North Core Banks (NCB). Black dots on the dune crest elevation plots represent years when new lidar was collected.

Tables

Table 1. Extreme or named storms within a 100 km radius of Cape Lookout National Seashore between 1997-2017. Storm categories represent extratropical storms (ET), tropical depressions (TD), tropical storms (TS), and hurricanes (categories 1–5 are denoted as H1-H5). The maximum total water level

(TWL) and still water level (SWL) that occurred within CALO for each event is provided. The percent of the total number of transects within the study region for which each storm was associated with the annual five largest TWL events at each location from 1997-2017 is provided in the last column. Grey rows highlight storms with one or more transects that identify the event as corresponding to the five largest TWL events per year.

Storm Number	Storm Name	Year	Month	Day	Storm Category	Max TWL (m)	Max SWL (m)	Transects (%)
1	Bonnie	1998	Aug	19-31	TS-H2	12.73	0.98	98 %
2	Dennis	1999	Aug-Sep	24-08	TS	7.49	1.04	90 %
3	Floyd	1999	Sept	07-19	H2	7.53	1.24	98 %
4	Irene	1999	Oct	12-19	H1	6.75	0.75	62 %
5	Allison	2001	Jun	05-19	TD	2.59	0.58	0 %
6	Arthur	2002	July	14-19	TD	2.58	0.56	0 %
7	Kyle	2002	Sept-Oct	20-12	TD	4.22	0.85	83 %
8	Isabel	2003	Sept	06-20	H2	10.30	1.09	97 %
9	Alex	2004	Jul-Aug	31-06	H1-H2	6.04	0.67	70 %
10	Bonnie	2004	Aug	03-14	TD	6.04	0.65	70 %
11	Ophelia	2005	Sept	06-23	H1	6.83	1.37	95 %
12	Barry	2007	May-Jun	31-05	ET	7.37	0.68	32 %
13	Gabrielle	2007	Sept	08-11	TS	7.37	0.61	26 %
14	Cristobal	2008	July	19-23	TS	3.54	0.6	0 %
15	Irene	2011	Aug	21-30	H1	9.84	1.26	95 %
16	Beryl	2012	May-Jun	25-02	TS	4.41	0.76	5 %
17	Arthur	2014	Jun-July	28-09	H2	7.45	0.87	74 %
18	Bonnie	2016	May-Jun	27-09	TD	2.73	0.92	0 %
19	Colin	2016	Jun	05-08	ET	2.42	0.89	0 %
20	Hermine	2016	Aug-Sept	28-08	TS	4.74	0.89	21 %
21	Julia	2016	Sept	13-21	ET	2.60	0.77	0 %
22	Matthew	2016	Sept	10-28	H1	2.89	0.83	0 %
23	Not Named	2017	Aug	27-29	TS	4.73	0.71	0 %

Table 2. (a) The coefficient of determination (R^2) for the average dune toe and crest elevations and the TWL impact hours per year (hpy), dune building hpy, and CDDF ratio for the single transect at km 5 on SHB, two-kilometer region between kms 19-21 on SCB, and a 20-kilometer area between kms 7-27 on

NCB between 1998-2016. Bold values represent coefficients that are statistically significant at the 95% confidence level. Grey values in parentheses represent the minimum and maximum R^2 values at the 95% confidence level for all single and two-kilometer averaged sections along SHB and SCB. (b) The percent of individual transects between kms 4-14 on SHB, kms 8-36 on SCB, and kms 7-27 on NCB with a statistically significant correlation between the dune toe and crest elevations and the TWL impact hpy, dune building hpy, and CDDF ratio. The values in parentheses for the dune building hpy represent the range of significantly correlated transects for varying dune building criteria (i.e., minimum number of consecutive hours for sediment entrainment, critical fetch length, and threshold velocity) (Supporting Information).

(a) Coefficient of Determination

Dune Toe Elevation (m)	Average TWL Impact hpy (R^2)	Average Dune Bldg hpy (R^2)	Average CDDF ratio (R^2)
SHB (km 5-5; 1 transect)	**0.51** **(0.21-0.67)**	**0.63** **(0.21-0.81)**	**0.75** **(0.21-0.77)**
SCB (kms 19-21; 50 transects)	**0.46** **(0.28-0.61)**	0.10 **(0.21-0.56)**	**0.46** **(0.21-0.62)**
NCB (kms 7-27; 500 transects)	**0.45**	0.04	**0.41**
Dune Crest Elevation (m)			
SHB (km 5-5; 1 transect)	0.20 **(0.21-0.66)**	0.01 **(0.22-0.77)**	0.13 **(0.21-0.69)**
SCB (kms 19-21; 50 transects)	**0.45** **(0.24-0.55)**	0.08 **(0.37-0.37)**	**0.44** **(0.31-0.55)**
NCB (kms 7-27; 500 transects)	**0.55**	0.05	**0.49**

(b) Percent of Transects with a Significant Correlation

Dune Toe Elevation (m)	TWL Impact hpy (%)	Dune Bldg hpy (%)	CDDF ratio (%)
SHB (kms 4-14; 250 transects)	60	52 (45-54)	69
SCB (kms 8-36; 700 transects)	54	58 (51-63)	58
NCB (kms 7-27; 500 transects)	61	53 (49-54)	63
Dune Crest Elevation (m)			
SHB (kms 4-14; 250 transects)	28	24 (22-25)	29
SCB (kms 8-36; 700 transects)	27	23 (21-25)	27
NCB (kms 7-27; 500 transects)	45	32 (31-33)	45

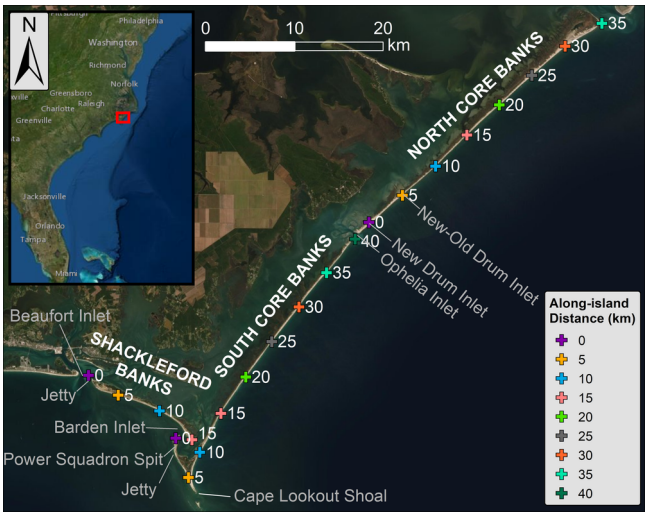

ESP_5210_Figure_1.tif

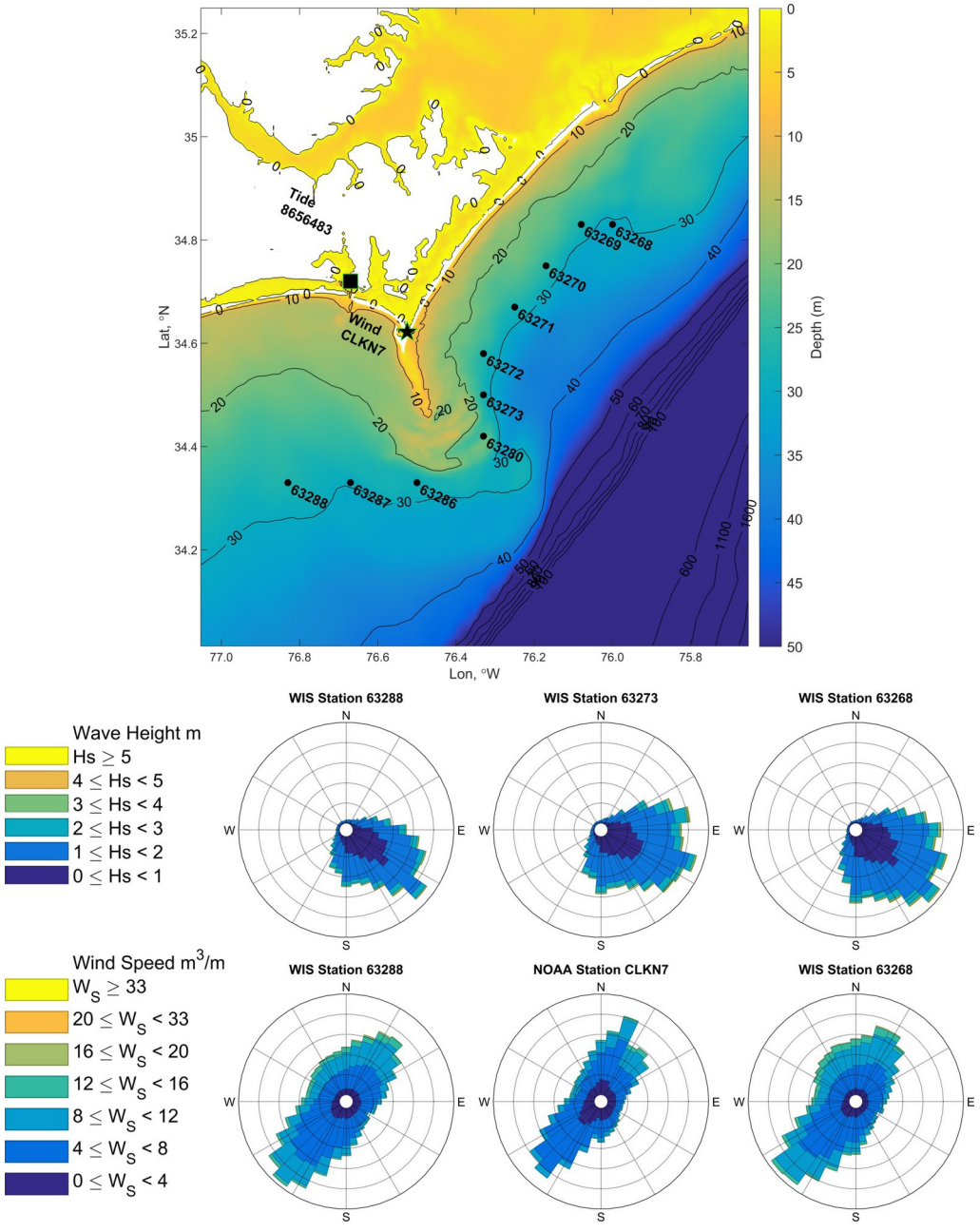

esp_5210_figure_2.eps

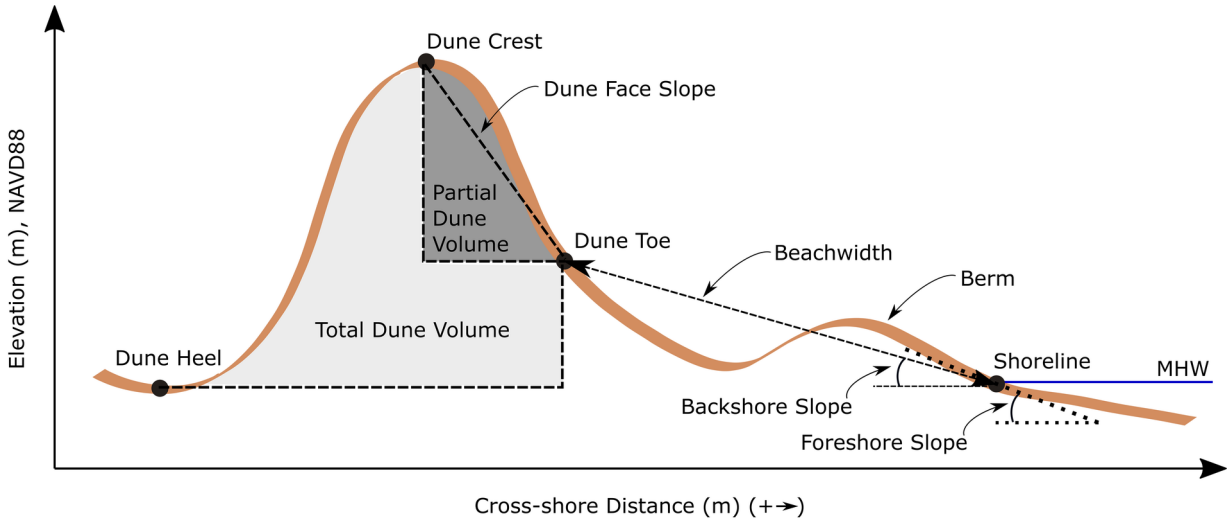

ESP_5210_Figure_3.tif

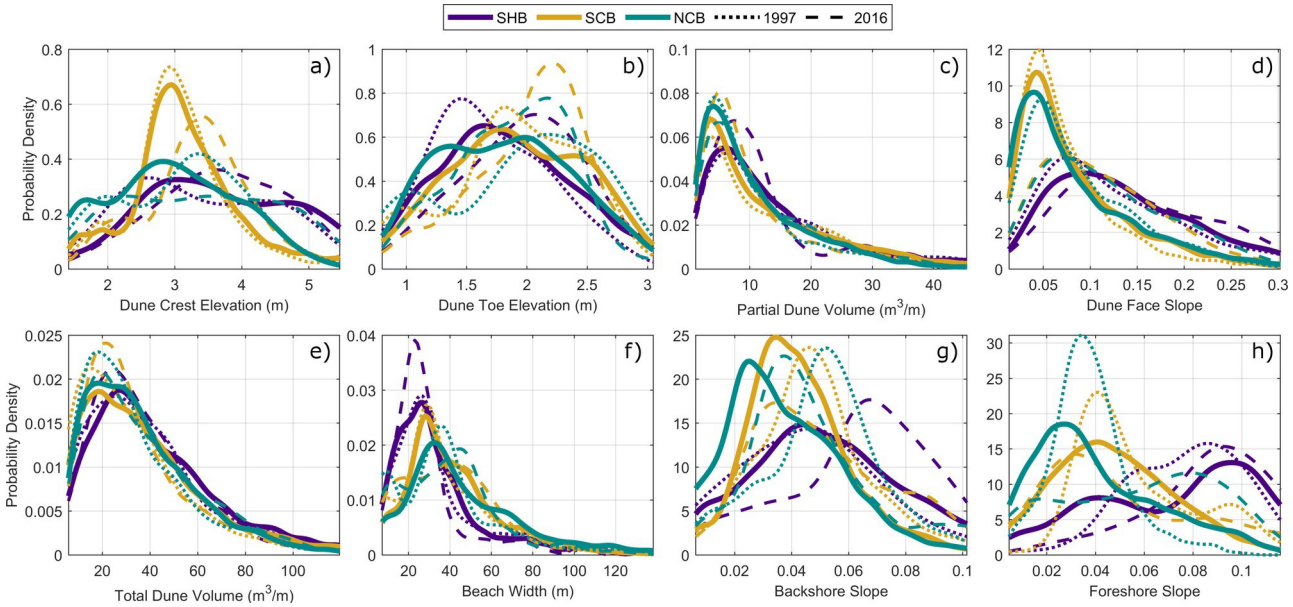

esp_5210_figure_4.eps

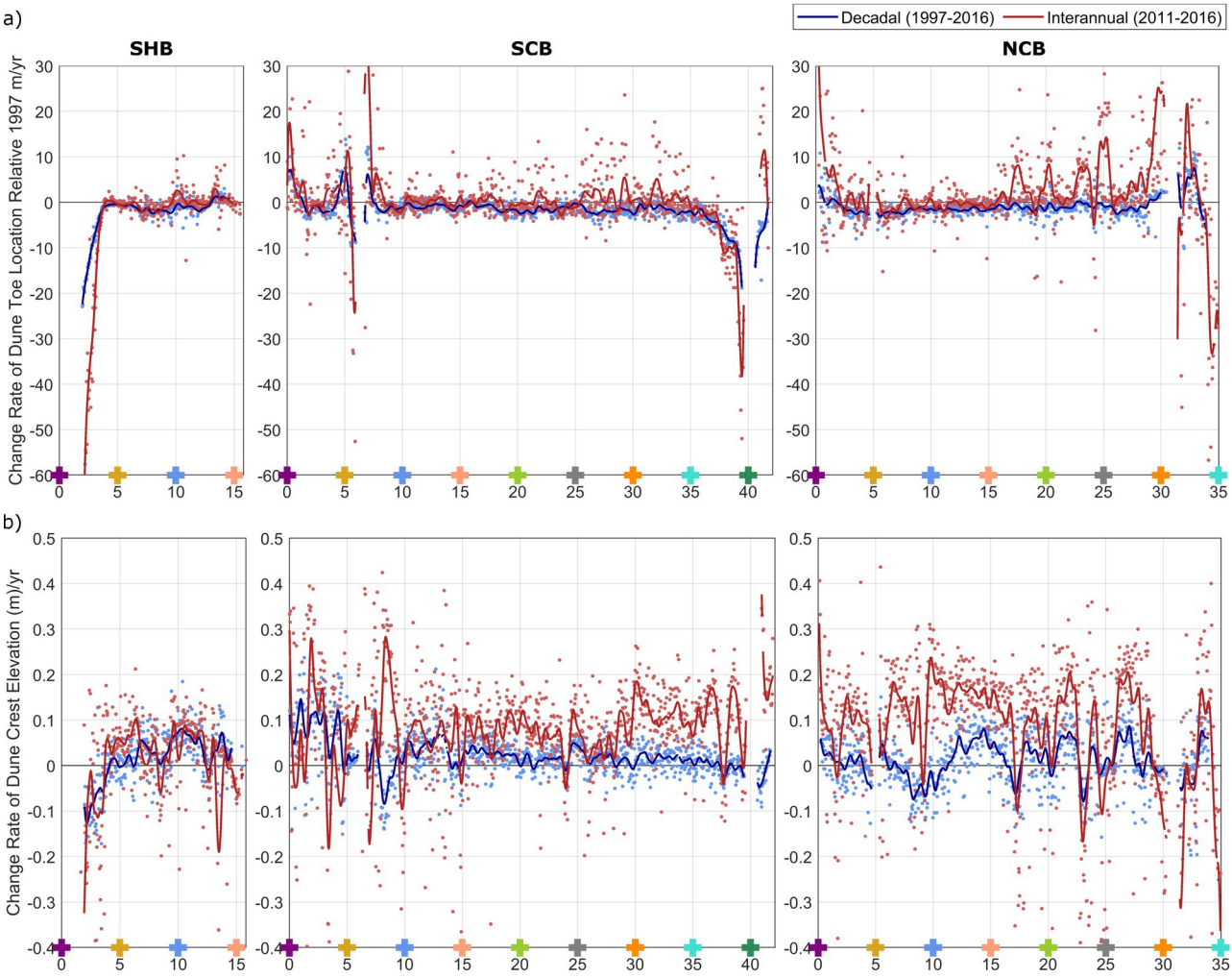

esp_5210_figure_5.eps

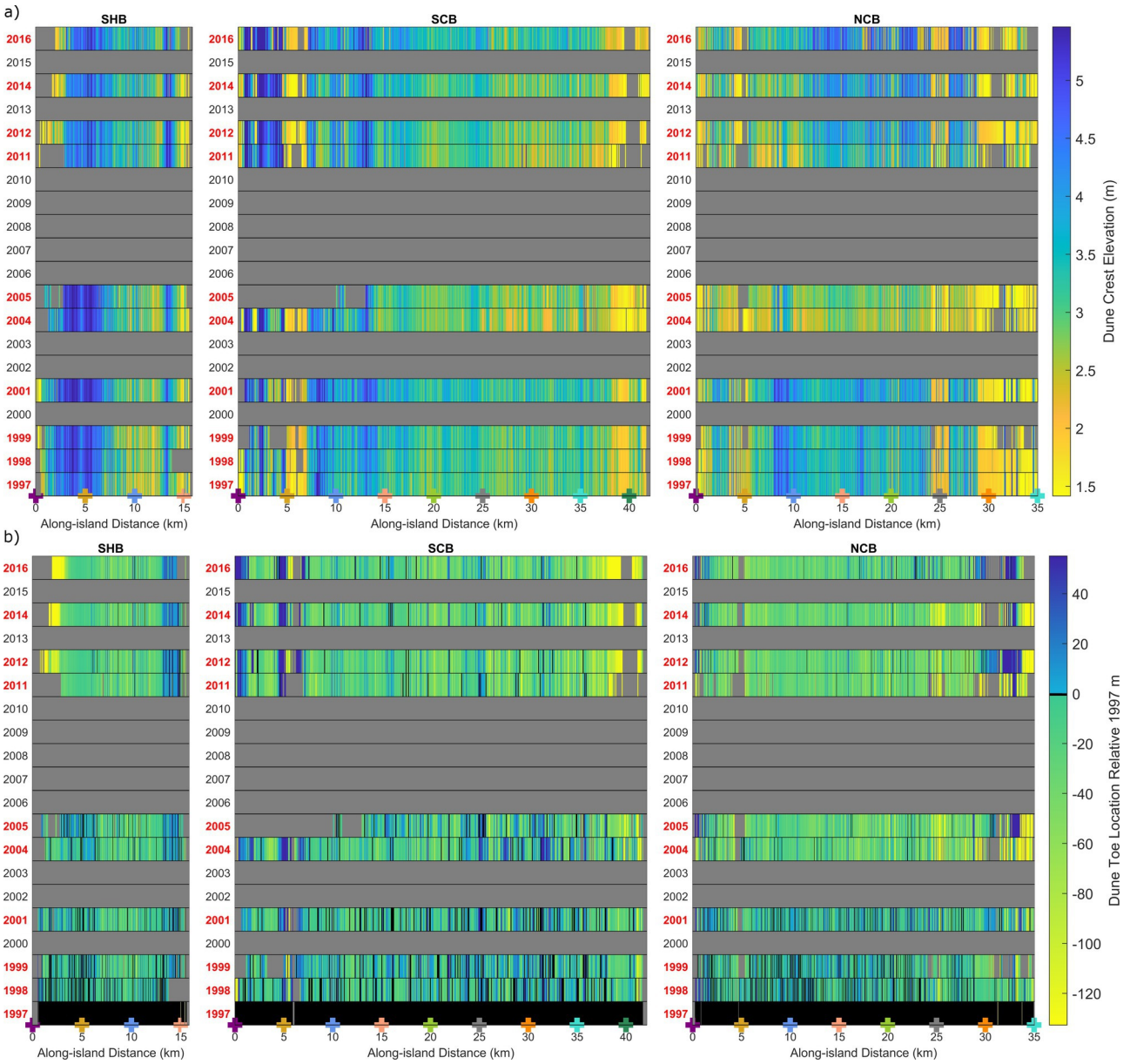

esp_5210_figure_6.eps

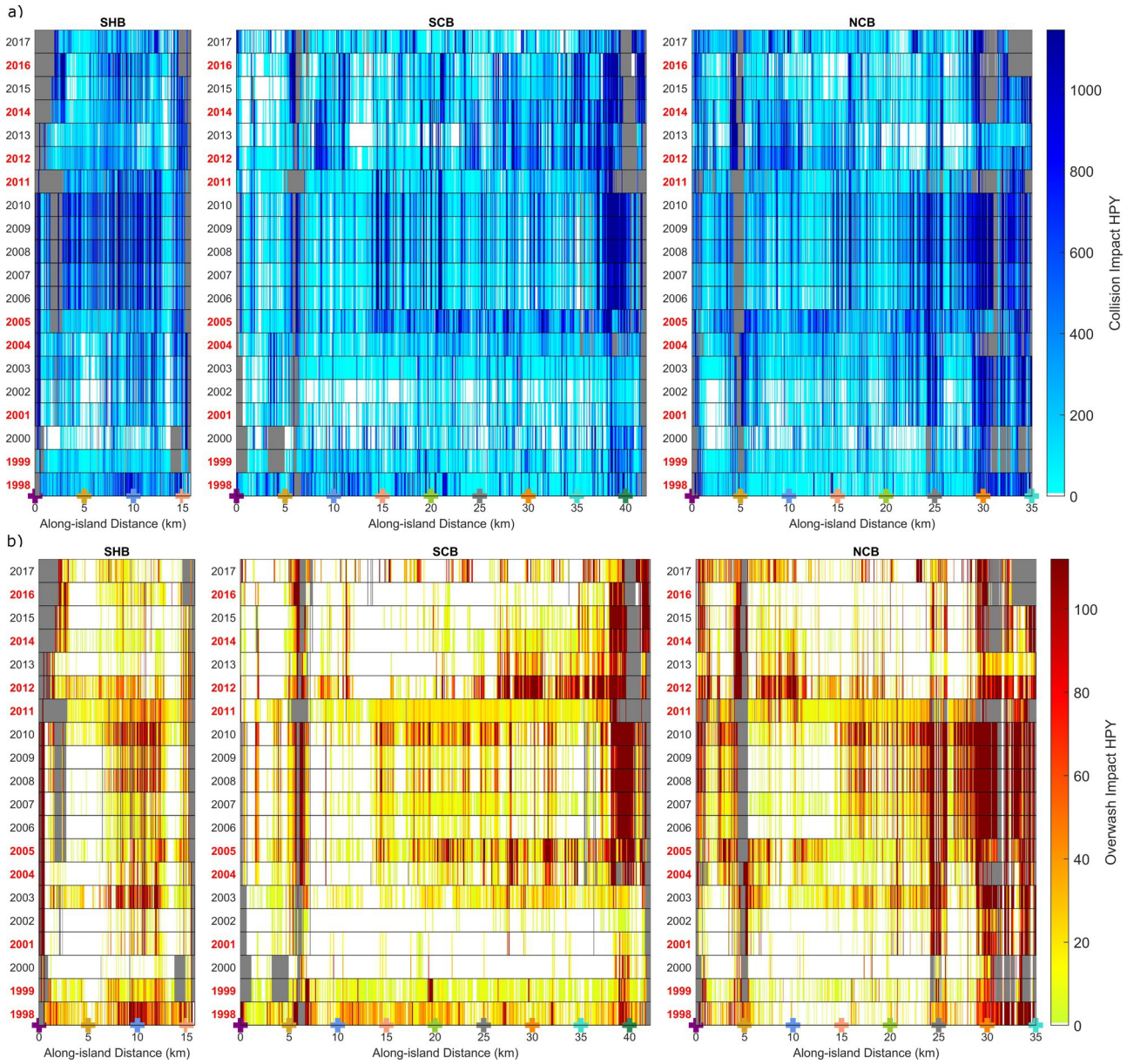

esp_5210_figure_7.eps

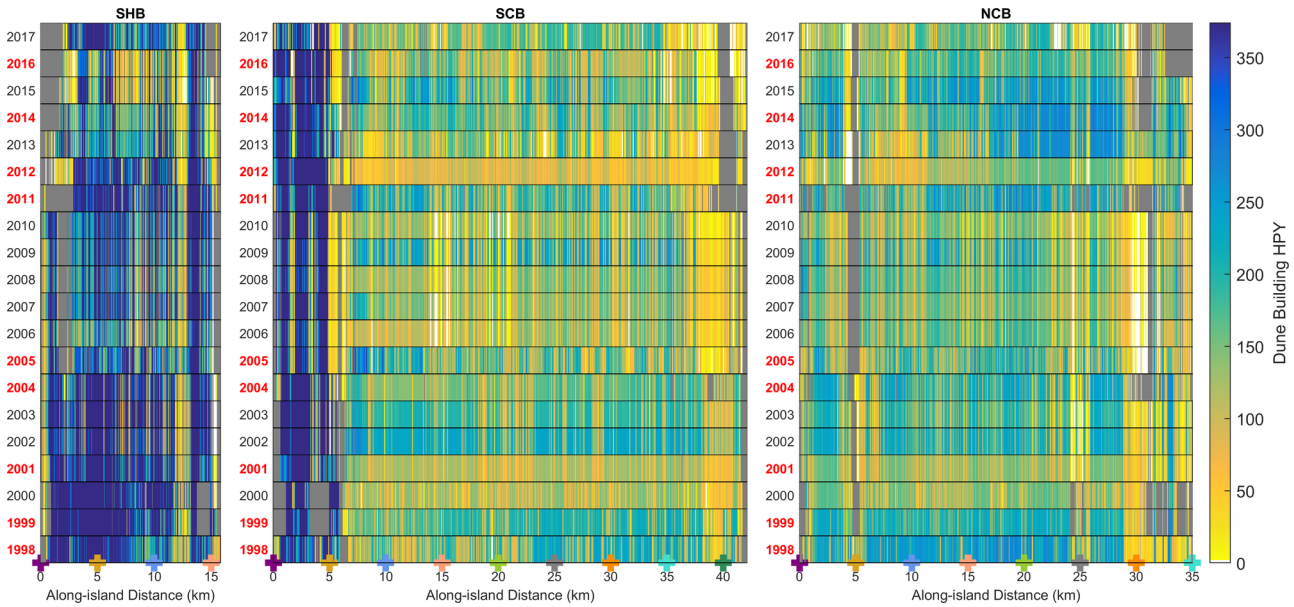

ESP_5210_Figure_8.tif

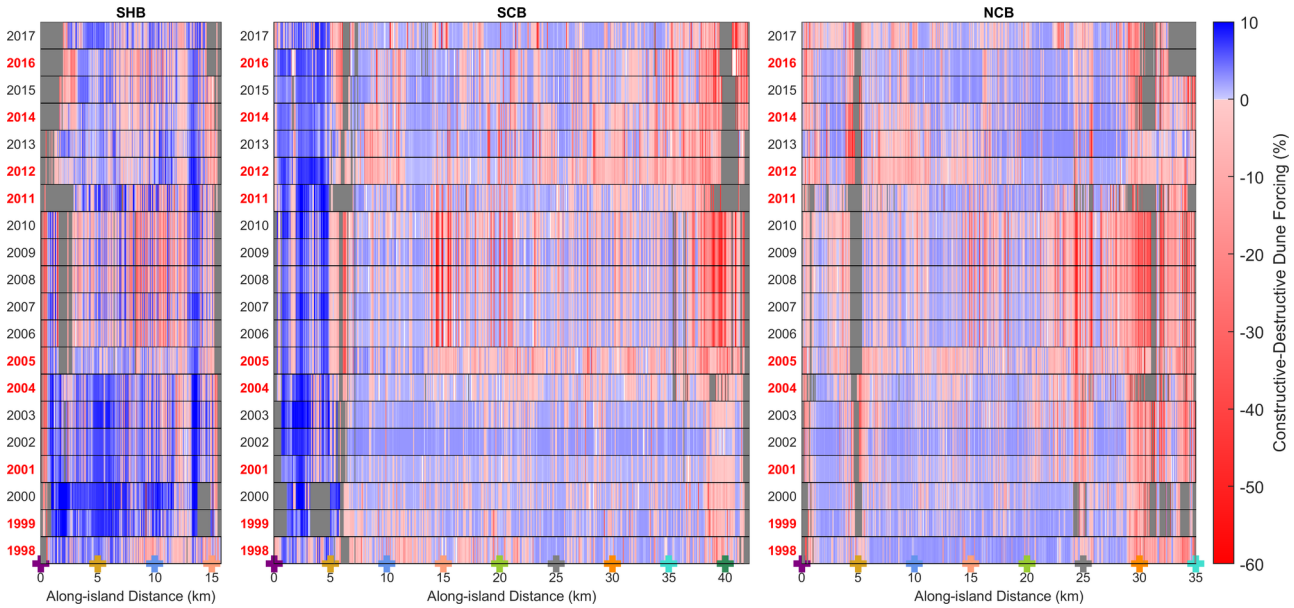

ESP_5210_Figure_9.tif

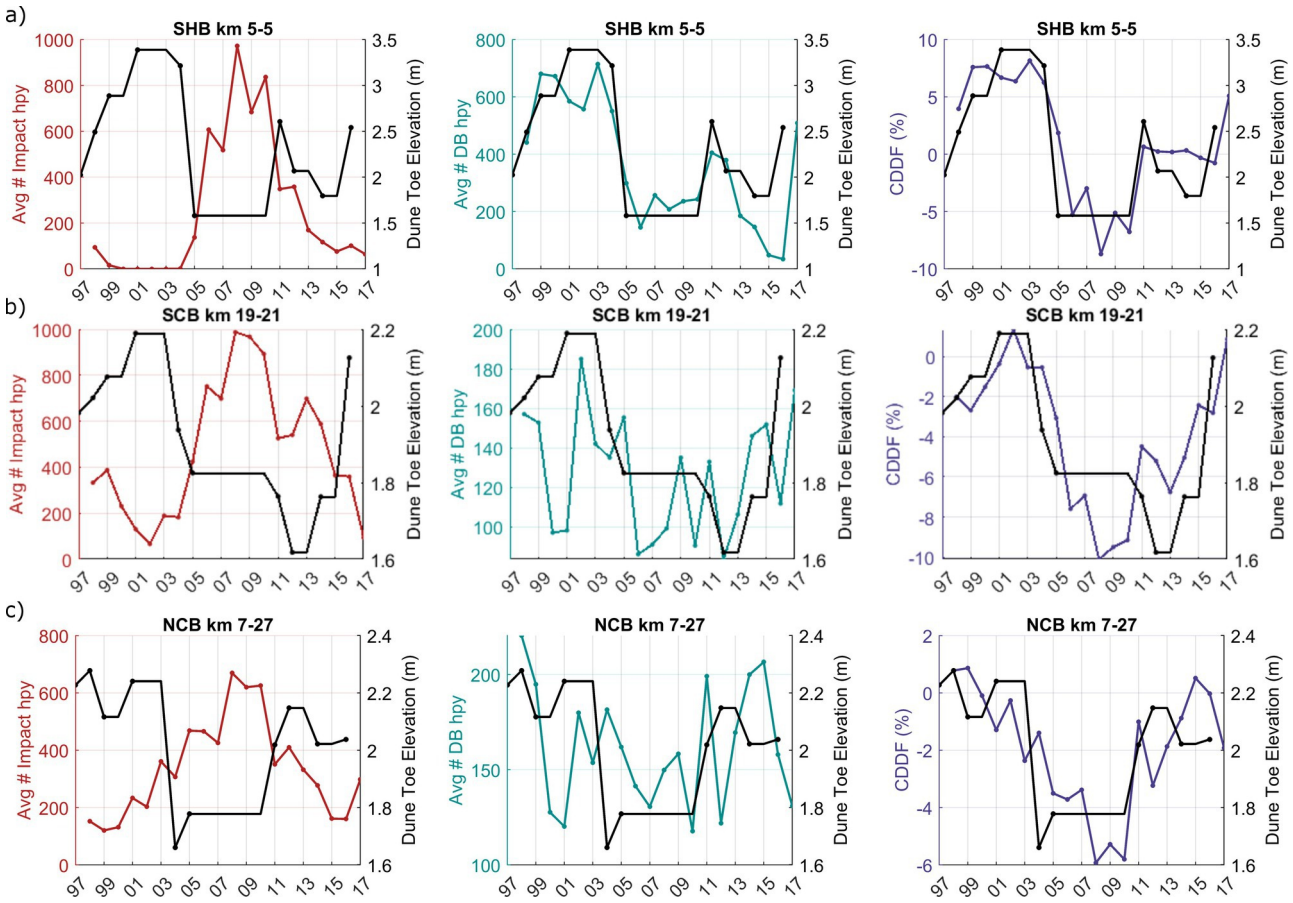

esp_5210_figure_10.eps

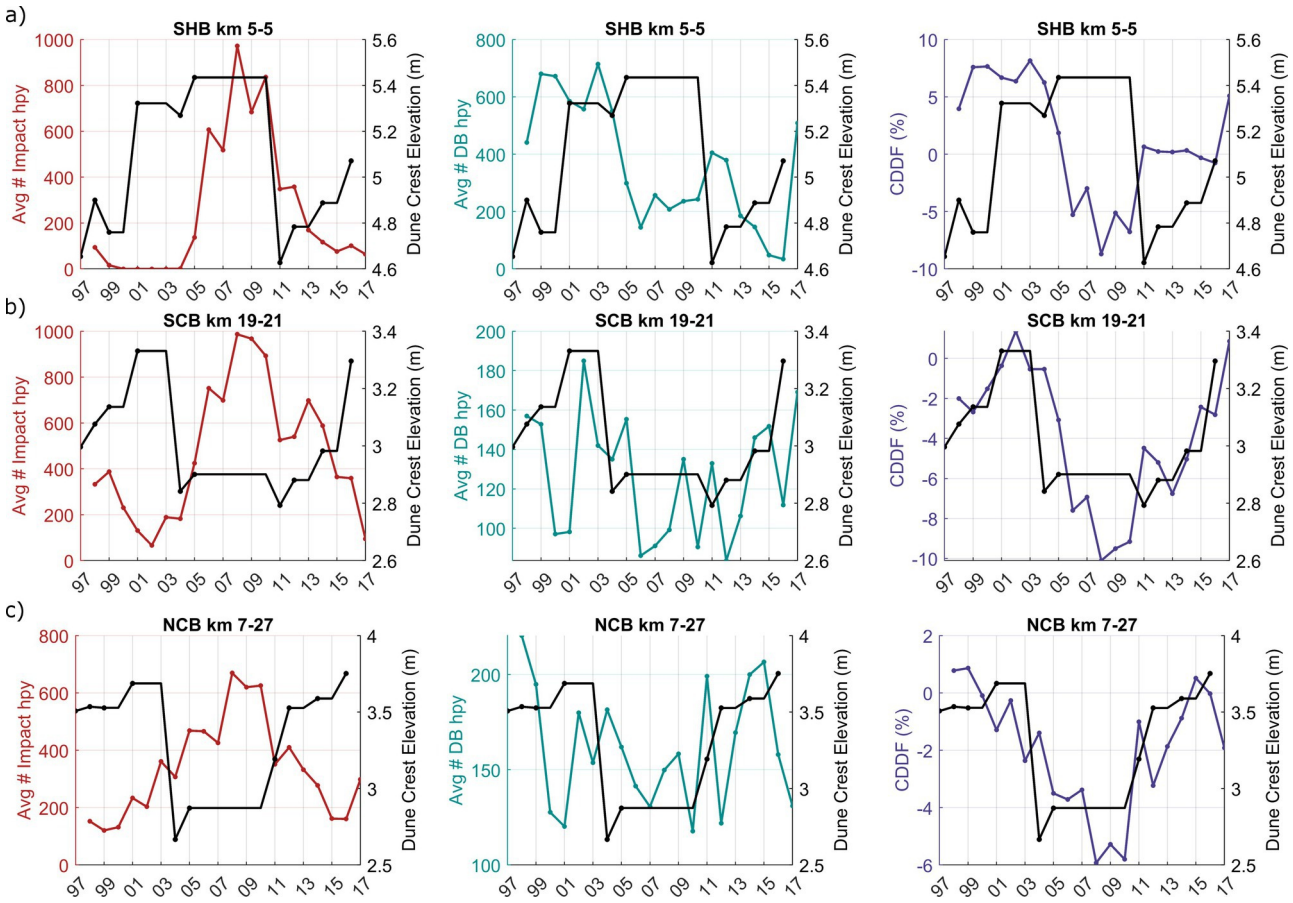

esp_5210_figure_11.eps